Escuela de Caminos
Escuela Técnica Superior de Ingenieros de Caminos, Canales y Puertos
UPC BARCELONATECH

TRABAJO FINAL DE MASTER

CONSEQUENCES OF GENDER INEQUALITY IN THE FACE OF EARTHQUAKE DISASTERS

Trabajo realizado por:

Ana Maria Zapata Franco

Dirigido por:

Yeudy Felipe Vargas Álzate

Máster en:

Ingeniería del Terreno

Barcelona, 11 de mayo de 2022

Departamento de Ingeniería Civil y Ambiental

Acknowledgments

First, thanks to my God for giving me life and health to live this great opportunity.

I would also like to sincerely thank the support, patience, advice, vision, and dedication of my tutor Yeudy F. Vargas A., who always guided me and shared his knowledge and ideas throughout this work. Special thanks to Dr. María Teresa Matijasevic for sharing her experience on issues related to the gender dimension in Colombia.

I would especially like to acknowledge the great love and unconditional support that I have always had from my parents, Luz S. Franco and Rommel Zapata, and my brother Juan J. Zapata, because with their support, advice, and constant motivation I have always been able to move forward. As well as my Spanish family Maria J. Quiroga and Mariano Llorente who opened the doors of their home to me, giving me great support, love, and motivation always.

I thank my friends, Rafa, Maria, Anibal, and Belen, for making this stage of my life a very pleasant experience.

Abstract

Research on women's exposure to various types of natural hazards has shown that gender inequality can increase their risk of being adversely affected. For example, in developing countries, people living below the poverty line are the most exposed to natural hazards; seventy percent of the global population living in this condition are women. In addition, many of them are housewives who are responsible for household chores and raising children, which means that they must stay indoors for longer periods of time, increasing the risk of being affected by catastrophic natural events. This is due to the fact that their homes are not built with the minimum seismic-resistant requirements to withstand an earthquake, making them vulnerable to collapse. For these reasons, this thesis seeks to estimate the consequences of gender inequality after a catastrophic seismic event for the five most important regions of Colombia. To do this, the time spent by women and men inside their homes was determined, using the 2017 National Administrative Department of Statistics (DANE) survey on time use. In turn, the exposure and seismic hazard of unreinforced masonry dwellings (URMM), which are commonly found in low-income areas of Colombian cities, was estimated. Based on this information and by performing probabilistic models in which it is necessary to obtain IM-EDP point pairs, characterized by a non-linear regression, will allow obtaining fragility curves for different states of damage. From these IM-EDP data, the Hazus 99 methodology was implemented to estimate the number of affected people discriminated by gender. The forecasts show that, in the event of a seismic catastrophe, women are more likely to be negatively affected than men.

Keywords: Gender inequality, social vulnerability, seismic risk scenarios, seismic risk assessment

Resumen

Las investigaciones sobre la exposición de las mujeres a diversos tipos de peligros naturales han demostrado que la desigualdad de género puede aumentar su riesgo de verse afectadas negativamente. Por ejemplo, en los países en desarrollo, las personas que viven por debajo del umbral de la pobreza son las más expuestas a los peligros naturales; el setenta por ciento de la población mundial que vive en esta condición son mujeres. Además, muchas de ellas son amas de casa que se encargan de las tareas domésticas y de la crianza de los hijos, lo que les obliga a permanecer en casa durante más tiempo, aumentando el riesgo de verse afectadas por fenómenos naturales catastróficos. Esto se debe a que sus viviendas no están construidas con los requisitos mínimos de resistencia sísmica para soportar un terremoto, lo que las hace vulnerables al colapso. Por estas razones, este estudio busca estimar las consecuencias de la desigualdad de género tras un evento sísmico catastrófico para las cinco regiones más importantes de Colombia. Para ello, se determinó el tiempo que pasan las mujeres y los hombres dentro de sus hogares, utilizando la encuesta de uso del tiempo del Departamento Administrativo Nacional de Estadística (DANE) de 2017. A su vez, se estimó la exposición y la peligrosidad sísmica de las viviendas de mampostería no reforzada (URMM), que comúnmente se encuentran en zonas de bajos ingresos de las ciudades colombianas. Con base en esta información y mediante la realización de modelos probabilísticos en los que es necesario obtener pares de puntos IM-EDP, caracterizados por una regresión no lineal, se podrán obtener curvas de fragilidad para diferentes estados de daño. A partir de estos datos IM-EDP, se implementó la metodología Hazus 99 para estimar el número de afectados discriminados por género. Las previsiones muestran que, en caso de catástrofe sísmica, las mujeres tienen más probabilidades de verse afectadas negativamente que los hombres.

Palabras clave: Desigualdad de género, vulnerabilidad social, escenarios de riesgo sísmico, evaluación del riesgo sísmico

INDEX

LIST OF FIGURES

LIST OF TABLES

CHAPTER 1: INTRODUCTION

1. Introduction

The 2030 Agenda for Sustainable Development has proposed 17 Sustainable Development Goals [1], SDG, to end poverty, fight inequality and injustice, build economic growth and address a range of social needs, while tackling climate change. The thirteenth goal points towards strengthening resilience and adaptive capacity to climate-related hazards and natural disasters worldwide. Natural Hazard (NH) issues are also shared by other goals like the ninth (Industry, Innovation, and Infrastructure), the eleventh (Sustainable Cities and Communities) and the fifteenth (Life on Land), since economical activities, infrastructures, people, and services are elements at risk. Protecting them is one of the facets for integrating gender equality measures in national policies, strategies, and plans, declared as the fifth goal of the SDGs.

Seismic risk mainly depends on the capacity of civil infrastructure to withstand ground motions produced by earthquakes. Current strategies to mitigate this inherent risk to society are oriented to improve design methodologies for new structures and to quantify the expected performance of existing ones. In turn, innovative technologies are implemented day by day to improve this performance.

Depending on the severity of an earthquake, and its proximity to human settlements, civil structures can be seriously affected. In this respect, due to world population growth, which exhibits higher rates in low-income regions, in a short time, there will hardly be a place where a moderate- to high-magnitude earthquake can occur without affecting society. In addition, increasing globalization has produced a redistribution of the risks to the entire society. That is, a couple of decades ago, negative consequences of catastrophes barely affected other areas than the stricken ones. However, because of immigration and commercial activities between countries, nowadays, this can no longer be affirmed. For all these reasons, the current risk associated to seismic disasters is higher than at any previous time, and if no proper measures are taken, it will continue increasing [2]. This can lead to the collapse of civil structures, injuries, casualties, not to mention that economic losses can affect the sustainable development of entire countries. These socioeconomic setbacks trigger poverty, inequality, amongst many other negative consequences. This should be a concern of the whole society and not only of the areas with high seismic hazard.

In addition to the above, gender inequalities can lead to an increased risk of injury for women. This can be explained if two main facts are considered:

1. An important amount of people living below the poverty threshold are women, [3];
2. In certain places, women living in vulnerable urban areas stay in their homes longer than men.

This increased risk has been evidenced by researchers from the London School of Economics and the University of Essex, who in 2007 carried out a study that counted the number of women who died in 141 countries during seismic catastrophes between 1981 and 2002 [4]. From this data, it was determined that during earthquake catastrophes, more women died than men, and the greater the magnitude of the event, the greater the gender gap. For instance, after the earthquakes that occurred in Maharashtra in 1993, which caused the death of approximately 10,000 people, and the one in Gujarat in 2001, with a total of 20,000 deaths, it was observed that one of the main factors that increased mortality in women was that they stayed most of the time inside their house, while the men were in open areas [5].

A similar case can be observed after the tsunami generated in the Indian Ocean in 2004, one of the most devastating so far, where a ratio of four women died for every man in the Aceh-Indonesian population was counted. This can be seen in Fig. 1-1, which shows the percentages of deaths during the tsunami, distinguished by age and gender. In this figure the largest gap was between the ages of 35 and 44 years, with a difference of approximately 15% between men and women [6]. Many of these deaths are attributed to the fact that women in these regions are not taught to swim or climb trees, reducing their chances of survival. In addition, after these events, many women were paraplegics because they were inside their homes at the time of the events, which caused many of them to be left by their partners, since they could not take care of their duties within the house or the care of the children.

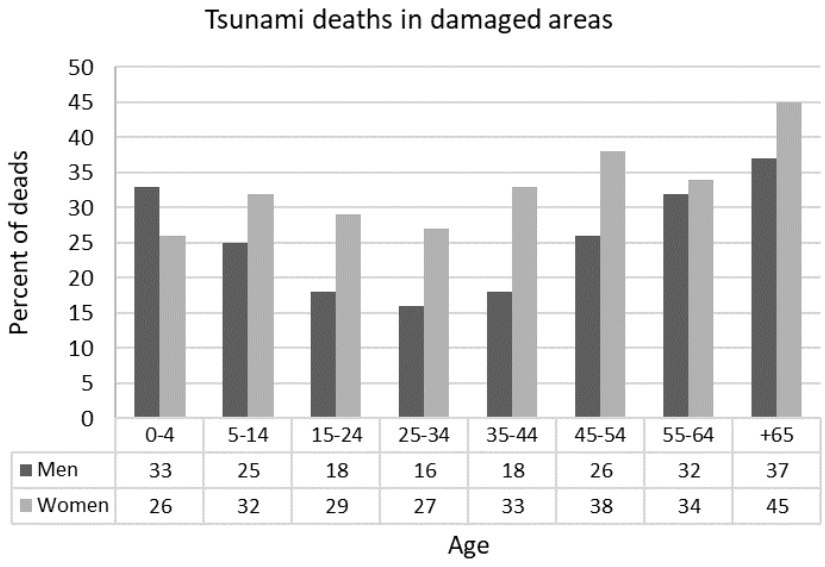

Fig. 1-1. Percentages of deaths during the tsunami were separated by gender ages [6].

This tendency has also been observed after analyzing the gender distribution of the people affected by an earthquake that stricken the coffee area of Colombia (on January 25, 1999, at 13:19 with a magnitude of 6.3 Mw), which released a significant amount of energy that seriously affected the infrastructure of the area and compromised the safety of the surrounding inhabitants.

According to the DANE's report on this event [7], it was quantified a total of 1,185 casualties, 8,536 injured, 35,972 houses were destroyed or uninhabitable and 4,467 houses were partially affected. It is worth mentioning that several of the affected dwellings were of the structural typology known as un-reinforced mid-rise masonry (URMM). Despite the high seismic vulnerability of this typology, it is very frequent in several urban environments in Colombia, even in areas where the seismic hazard can be considered moderate-to-high.

Out of the total number of casualties during the catastrophe, 78% were concentrated within the city of Armenia. At that time, the city had a total of 214,388 inhabitants, of which 101,166 were men and 113,222 were women. During the emergency, a total of 921 casualties and 383 disappeared were reported. In the case of men, a total of 445 casualties and 128 disappearances were informed, while on the women's side these numbers were 476 casualties and 255 disappearances.

In low-income areas, the unbalance can be explained by the fact that women stay at home longer than men. This is because dwellings in these areas are commonly built without regard to regulations and, what is worse, in high-risk locations. Evidence of the unequal distribution of time to perform domestic activities can be found in a survey conducted by the National Administrative Department of Statistics of Colombia (DANE by its acronym in Spanish) aimed at quantifying the amount of time spent on daily activities by Colombian citizens [8].

This situation has triggered the need for governments around the world to create new strategies, in which they seek to reduce the risk of disasters. This situation has triggered the need for governments around the world to create new strategies, which seek to reduce the risk of disasters by promoting the care of women, ensuring their survival and recovery more efficiently. One of the countries with the best development of this program is Japan, with a score of 80.6 out of 100 according to the Women Resilience Index [9], while Pakistan has one of the lowest ones with 27.8. In Latin America, Chile has been one of the pioneers in the implementation of a new program after the 1960 earthquake in Valdivia to reduce the impact it could cause on women, which allows demonstrating that in this area the situation of gender inequality is opposite in comparison to other countries [10].

In Colombia, the National System for Disaster Prevention and Attention has been rising new programs to reduce seismic risk, in which local governments hire and train mothers to help implement risk mitigation activities, in addition to the managing of waste, maintenance of cleanliness of evacuation roads and riverbeds [11]. It is worth mentioning that women have a better understanding of what women need, thus, their involvement and leadership in disaster decision making is crucial [12]. In addition, this will allow the women of this area greater

independence, since they have their income, while they will have a greater knowledge of how to act in the event of a catastrophe of any kind.

1.1. General objective

The main objective of this thesis is to give a better visualization of the current situation of women facing seismic catastrophes, from the civil engineering point of view. It also seeks to contribute to goal number 5 of the Sustainable Development Goals [1], which pursues to give greater recognition and value to the care and unpaid work carried out by women within each household, through the implementation of new social policies and the improvement of infrastructure. To do so, it will be quantified the consequences of gender inequalities in the face of seismic disasters at urban level. Several regions of Colombia will be analyzed as a case study.

1.2. Specific objectives

In the following, a series of specific objectives are presented, aimed at increasing the efficiency to predict the number of affected by gender, including the main sources of uncertainty, refining methodologies to estimate the risk in a multi-hazard framework and analyze social aspects that influence the consequences of catastrophic events:

- Account for the time spent at home by Colombian's women performing unpaid domestic work.
- Carry out a selection of seismic records belonging to the Colombian territory, to adequately characterize the seismic hazard.
- Develop a simplified model to analyze the dynamic behavior of URMM structures, which are found in much of the country, in addition to being one of the most vulnerable structural typologies.
- Investigate and implement methods for risk assessment.
- Consider uncertainties affecting the dynamic response of the selected structural typology using the Monte Carlo method.
- Quantify the probability that women will be affected during a seismic catastrophe.

1.3. Methodology

This thesis seeks to create a simple representation of a complex reality, allowing to estimate the number of affected people by gender in an area after occurring a seismic event. This has been done using computational tools that allow many calculations in a short time.

To begin with, it is necessary to account for the time spent by both women and men in domestic activities. This information has been taken from a national time-use survey conducted in 2017 by DANE [8]. Then, it has been created a database of the most relevant earthquakes in the territory to properly characterise the seismic hazard. Specifically, it has been analyzed a large set of ground

motion records provided by the Colombian Geological Service (SGC) [13]. Note that the ground motion records obtained from the SGC must undergo a process of filtering, baseline correction and scaling; a computational program has been developed to this end. For scaling and selecting the records, the methodology presented in Vargas-Alzate et al. [14] has been used herein. Once these records have been identified, a set of intensity measures (IM) have been calculated.

To characterize the vulnerability and fragility of the URMM structures, it has been decided to employ the combined response of a set of single-degree-of-freedom (SDoF) systems. This type of models allows the time-history response of the structure to be obtained with less computational effort by solving the dynamic equilibrium equation. To account for plastic damage, and the participation of higher vibration modes, the dynamic response has been approximated by averaging the response of a set of SDoFs around the fundamental period of the simulated structures [15]. This period has been obtained through classical relationships in terms of power functions (see for instance Goel et al. 1997 [16]) which depend on the height of the structure.

Once the structural models have been obtained, the next step has been to calculate engineering demand parameters (EDP) that can be used to obtain fragility curves. These EDPs have been estimated by considering that the fundamental period of the structures randomly varies. Then, clouds of IM-EDP points in the log-log space have been used to identify the most efficient IM.

Once the most efficient IM has been identified, fragility functions have been derived for the URMM structural typology [17]; cloud analysis [18] has been used to this end. In brief, a regression line is obtained from the IM-EDP relationship, which is used to calculate the mean value of a parametric statistical distribution given an IM. The variation of this distribution is estimated from the standard deviation of the IM-EDP set with respect to the fitted curve, allowing to calculate the probability of exceeding a given damage threshold.

Once the variables described have been properly characterized, it has been possible to estimate the number of people that can be potentially affected after a seismic catastrophe. This calculation has been made using the Hazus methodology [19], which has been adapted to the purposes of this study. That is, data related to the probability of suffering an injury level, the probability of being woman or man, the probability of being at home (which is a key term since it modifies the probability of being negatively affected in a catastrophic scenario), and the number of people considered for the analysis have been considered in the calculation. In this way, it has been possible to count the number of affected people disaggregated by gender.

Finally, to validate if the results obtained are in line with reality, a comparison has been made using the reports related to the seismic catastrophe that occurred in 1999 in the coffee region of Colombia [7].

It is hoped that, based on the results obtained from this study, greater awareness can be generated about the danger that women face by staying longer in a dwelling considered vulnerable to seismic events. It is also expected that the methodological aspects developed in this thesis can be extended to other countries, where new strategies based on the quantification and mitigation of seismic risk can be implemented.

CHAPTER 2: BASIC CONCEPTS

2. Introduction

This section briefly describes the basic concepts required for the development of this study. A list of references on each aspect to further clarify some of them are also included herein.

2.1. Natural Hazard

Refers to the probability that a natural phenomenon of great magnitude and destructive potential may occur in a specific place and within a specific time interval. According to the National Risk Index [20], natural hazards are represented in terms of Expected Annual Loss. This includes data on exposure, annualized frequency and historical loss rate and can be classified into 18 groups:

- Avalanche
- Coastal Flooding
- Cold Wave
- Drought
- Earthquake
- Hail
- Heat Wave
- Hurricane
- Ice Storm
- Wildfire
- Winter Weather
- Volcanic Activity
- Strong Wind
- Tornado
- Tsunami
- Landslide
- Lightning
- Riverine Flooding

It is important not to confuse the terms natural hazards with natural disasters. When we speak of natural hazards, we refer to the threat of an event that is likely to have a negative impact. While if we talk about natural disasters, we refer to the negative impact that occurs after the occurrence of a natural hazard in case it affects a society.

2.2. Seismic hazard characterization

Seismic hazard refers to a value of future earthquakes at a given site. It is quantified in terms of ground acceleration and the probability of exceeding it in each period. To perform a seismic hazard assessment, the application of the classical theory of seismology was made considering the seismicity of the sources, as well as the laws of energy attenuation in relation to distance and the probability of expected seismic intensities. Based on this, it has been possible to estimate the probable seismic hazard for different points in Colombia.

Seismic hazard can be obtained by means of several methods. However, if enough information on the expected occurrence of seismic events is available, two main methods are frequently used:

- Probabilistic Seismic Hazard Analysis (PSHA): This type of analysis allows to consider the uncertainties related to the size, location, recurrence rate and the effects of the earthquake within the evaluation of the seismic hazard. In addition to this, this methodology allows generating a balance between the risk and the cost of the project. In the PSHA, the frequency of occurrence of the earthquake is directly incorporated, which means that for the regions that have greater seismic activity, there will be higher levels

of ground movement for certain return periods and probabilities. In this same way, the uncertainty of the location of the earthquake is incorporated, avoiding assuming that it will occur in the location closest to the source [21]. After the application of this method, the exceedance rate for a certain level of ground motion is obtained.

- Deterministic Seismic Hazard Analysis (DSHA): This method is mainly based on historical earthquakes, which means that future earthquakes will be generated in a similar way to past ones. To apply this method, source characterization is required which includes the identification and characterization of all seismic sources that can cause significant ground motion in the study area. Following this, the shortest distance between the source and the site of interest must be selected, as well as the selection of the control earthquake, that is, the earthquake that is expected to produce the highest level of movement. From these data, the hazard is defined in terms of earth movements produced by the earthquake that controls the site [21]. At the end of the analysis, the ground motion produced by the earthquake taken as reference is obtained.

A proper seismic hazard characterization is of utmost importance since it constitutes a tool for planning, risk estimation and helps to make better decisions to prevent risks caused by earthquakes. In terms of design, this will result in a greater durability of the project.

2.3. Seismic vulnerability

The term seismic vulnerability can be defined as the degree of loss of an element after a seismic event occurs [2]. The application of this methodology allows seismic risk management to be carried out, while at the same time helping to reinforce the built environments before the earthquake [22].

While the seismic hazard is estimated from the characteristics of the soil and the expected ground movements, the seismic vulnerability is estimated from the quality of the structure and the methods used for its construction. There are three methods that are considered the textbooks for vulnerability assessment [23]:

- Empirical techniques which are based on the damage observed after earthquakes.
- Analytical techniques employ the mechanical properties of a particular parameter, such as drift between stories.
- Hybrid techniques are a combination of empirical and analytical approaches.

2.4. Single Degree of Freedom

Perform analysis and design of structures to resist the effects of earthquakes requires the development of concepts that allow the simplification of the physical system, in an idealized system represented by a mathematical model [24]. The latter is carried out from independent

coordinates in which the position and configuration of the model is specified at each moment. This is known as degrees of freedom. Structures, being continuous systems, have infinite degrees of freedom.

The realization of these very specific models requires a high degree of computational effort. Therefore, the oscillator implementation of the single degree of freedom system is chosen to simplify the calculations. This oscillator is characterized by elements such as the mass and inertia of the structure, a spring k representing the elastic restoring force and potential energy capacity of the structure, a damper c representing frictional characteristics and energy losses. of the structure. structure and an exciting force F(t) representing the external forces acting on the structure [24].

2.5. Intensity measure (IM)

It is called as intensity to the measure recorded in different areas, after a seismic movement. This varies from place to place and depends mainly on the distance from the fault rupture area. The intensity can also vary, depending on the effects of the earthquake and the ground, such as the rupture direction and the type of geology that is in the area [25]. The IM contains relevant information to predict the seismic response of a structure.

Previously, intensity measurements were estimated subjectively, obtained from human observations, motion reports, and felt damage. However, currently, from the instrumental data obtained from each station, more accurate measurements of intensity can be obtained.

2.6. Engineering Demand Parameters (EDP)

EDP's can be described as structural response quantities that can be used to predict damage to structural and non-structural system components given an intensity measure (IM) of the ground motions [26]. Some of these parameters such as inter-story drift or story acceleration, can be correlated with structural, non-structural, and content damage within a structure [27]. Before the implementation of FEMA 273 [28], these parameters were limited only to the forces of the components and the displacements between floors. These became the basis for contemporary codes such as ATC-14 [29] and ATC-22 [30].

The corrections between the EDPs of the structures are mostly affected by the correlation between the IMs and the correlations between the residuals. The correlation with the IM is important for the empirical seismic attenuation residuals, while the correction between the EDP residuals is related to the uncertainty in the structural response, which does not depend solely on the selected IM [31].

2.7. Accelerograms

Accelerograms are a representation of the time evolution of the acceleration due to the Earth's motion. Measuring instruments called accelerometers, which measure conventional seismic signals in three directions (1 vertical and 2 horizontal), are used to obtain the acceleration [32].

It should be noted that all seismic signals contain noise, i.e. signals that are independent of the signals generated by earthquakes, such as the passage of vehicles, rivers, or neighboring buildings, measuring instruments, so it is necessary before using the seismic record or accelerometer to perform a study, a series of corrections and filtrations in it.

2.8. Fragility Curves

Fragility curves are defined as the probability of reaching or exceeding a specified damage state under earthquake excitation [33]. These are established as the proportion to predict the damage potential during an earthquake. In addition to this, it is used to reduce damage costs and reduce loss of life during seismic catastrophes. This allows the fragility curves to be used both for decision making before and after a seismic event.

The brittleness curves are obtained from the relationship between the intensity measure (IM) and the damage measure (DM) of structural and non-structural elements, representative of the group of structures to be studied. The curves can be defined as a function of the EDPs, and then be correlated with the IM from a structural model. These are selected because they are well correlated with the damage variables [34].

2.9. Response spectrum analysis

Response spectrum analysis is a non-deterministic method to estimate the structural response to seismic events. It can be represented in terms of acceleration, velocity, or displacement.

A response spectrum can be a function of frequency or period, where the maximum response of a simple harmonic oscillator that is subjected to a movement, in this case seismic, is represented. In addition to this, the spectrum is a function of the natural frequency of the oscillator and the damping. So, it is not a direct representation of the frequency content of the excitation (as in a Fourier transform), but of the effect that the signal has on a postulated system with a single degree of freedom (SDOF) [35].

CHAPTER 3: GENDER INEQUALITY

3. Introduction

Gender equality is a multidimensional term that equally encompasses economic, cultural, and social dimensions. The SDGs are one of the main strategies that are actively committed to gender equality. They offer an opportunity to promote human rights, advance gender equality and achieve health for all.

Disasters are gender neutral, but impacts are not. Men and women face different levels of disaster risk and vulnerability based on gender and discrimination. Disasters disproportionately affect women, including life expectancy, unemployment, re-entry into the labour market, and related property loss [36]. Gender inequality is intensified in crisis situations. To this end, new strategies have been proposed, including achieving gender equality and the empowerment of all women and girls, promoting sustained, inclusive, and sustainable economic growth, full and productive employment, and decent work for all, making cities and human settlements inclusive, safe, resilient, and sustainable. Although it may vary from one country to another, there are certain common aspects that will be the subject of debate in the coming years. [37]

3.1. Study of gender inequality

Currently many women are at a disadvantage in relation to men not only in labor and economic issues, but also in the way they are affected after a catastrophe. Women are thought to be more likely to die in disasters. This can be observed in less developed countries, where more deaths have been recorded in women than in men, after a natural disaster occurs [36]. Although men are associated with rescue and risk management professions, gender inequalities in access to preparedness information, access to public shelters, and reduced mobility appear to contribute more to gender-based mortality, putting disadvantaged women.

In contribution to the study of gender inequality, different authors have shown that the difference in the mortality rate between men and women is not only attributed to their biological and physiological conditions, but also to external factors such as natural disasters, generate a contribution to the increase of this gap [38].

Neumayer in his article “The Gendered Nature of Natural Disasters: The Impact of Catastrophic Events on the Gender Gap in Life Expectancy, 1981–2002” [4] analyzed the effects of the forces of the disaster. From this study, the following statements were obtained:

- Natural disasters reduce the life expectancy of women compared to men.
- The larger the scale of the disaster, the greater the gender gap, in which women are the most affected.
- The higher the socioeconomic level of women, the lower the mortality rate.

Understanding how disasters arise from violence against women and girls is more important than ever for gender-sensitive policy making in disaster management [39].

3.2. Gender inequality in Colombia

Throughout history and especially in recent years, women have been proposed to play a central role in addressing issues related to global problems, such as poverty, health, and climate change. Women have taken it upon themselves to work tirelessly to promote health, education, and environmental sustainability programs [40].

On the other hand, women face many obstacles in the way of achieving gender equality. Colombia has until recently been hit hard by decades of violent armed conflicts that have had a significant impact on the country's general society. Today, peace processes bring new hope to the country, however, some social problems remain.

One such issue is that gender inequality systematically hampers women's ability to advance and reach their full potential. Colombia should be a country where men and women are treated equally and fairly, instead, women's rights have always been affected by violence, social exclusion, exploitation, and discrimination. Gender inequality creates a major barrier to overcome for women who want to make an effective contribution to the much-needed development in Colombia [40].

3.3. Time spent on daily activities

Historically, women have fulfilled the role of caregivers within the home. Nowadays, in several places across the planet, they are still in charge of a large part of domestic activities related to cleaning, food preparation, childcare, amongst many other activities that are not economically remunerated. Performing these activities does not allow many of them to have enough time to generate their own income or develop professionally. Furthermore, women living in low-income regions may be disproportionately affected by this unbalance. This is because their homes are generally at high-risk in front of natural disasters, and they remain more time at home than men. In this respect, between 2016 and 2017, DANE conducted a survey of people from 44,999 households, which sought to collect information related to the formation of households, type of housing and the number of people who lived in them [7]. As an added value to this survey, people were asked about the time spent on housework, personal care, passive, and other unpaid care. This questionnaire was designed in this way to get people's opinion on gender roles.

This survey was conducted considering various regions of the country. Thus, the results were classified according to each region. In general, it was observed that women spend more time in domestic activities than men. In the present study, five regions of Colombia were taken as reference to perform the analysis.

The unpaid domestic activities have been used to determine the time spent at home of citizens in this area. The following ones have been considered in this thesis:

- A1. Food supply
- A2. Wardrobe maintenance
- A3. Home cleaning and maintenance
- A4. Activities with children under 5 years of age
- A5. Physical care for people at home
- A6. Support for household members
- A7. Personal care, including sleep

From the data provided by DANE [8], Fig. 3-1 presents the average and the total time in minutes spent at home within each region, separated by activity and gender. Based on these data, the dedication ratios were estimated for each of the activities and regions, comparing the time spent by women and men, as shown in Table 3-1.

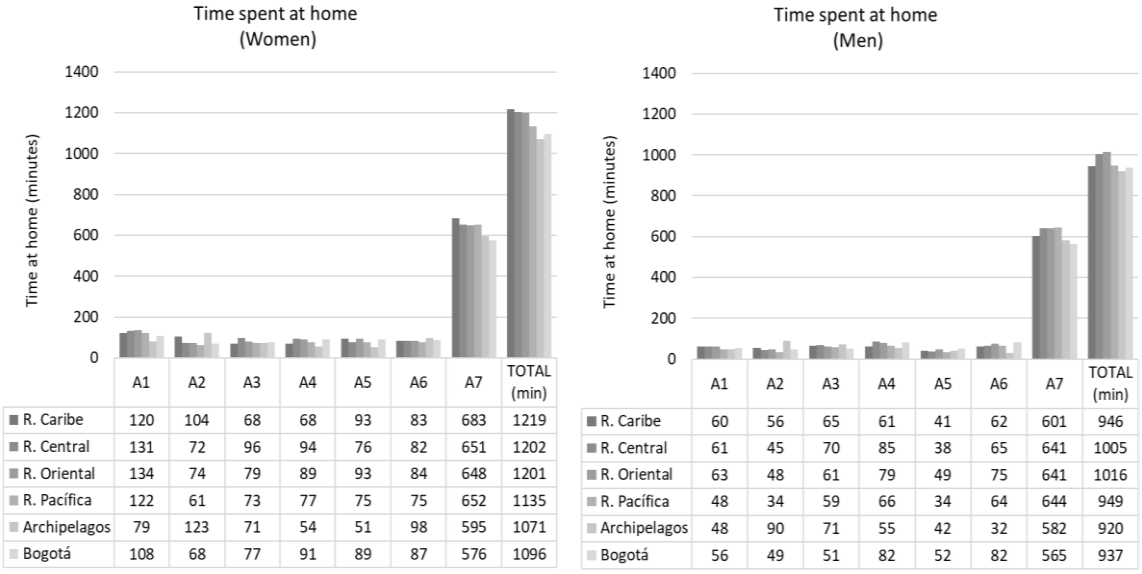

	A1	A2	A3	A4	A5	A6	A7	TOTAL (min)
R. Caribe	120	104	68	68	93	83	683	1219
R. Central	131	72	96	94	76	82	651	1202
R. Oriental	134	74	79	89	93	84	648	1201
R. Pacífica	122	61	73	77	75	75	652	1135
Archipelagos	79	123	71	54	51	98	595	1071
Bogotá	108	68	77	91	89	87	576	1096

	A1	A2	A3	A4	A5	A6	A7	TOTAL (min)
R. Caribe	60	56	65	61	41	62	601	946
R. Central	61	45	70	85	38	65	641	1005
R. Oriental	63	48	61	79	49	75	641	1016
R. Pacífica	48	34	59	66	34	64	644	949
Archipelagos	48	90	71	55	42	32	582	920
Bogotá	56	49	51	82	52	82	565	937

Fig. 3-1. Time spent in activities at home by region and the total time in minutes

It has been determined that the length of stay of women in each of the regions is in a range of 1.16 to 1.29 times, with the Caribbean region being the one that spends the most time with women in the home and the Archipelagos the least. As previously mentioned, this imbalance has consequences in the estimation of seismic risk.

Table 3-1. Dedication ratio by regions

Activities	Dedication ratio					
	Caribe	**Central**	**Oriental**	**Pacifica**	**Archipelagos**	**Bogotá**
A1	2,00	2,15	2,13	2,54	1,65	1,93
A2	1,86	1,60	1,54	1,79	1,37	1,39
A3	1,05	1,37	1,30	1,24	1,00	1,51
A4	1,11	1,11	1,13	1,17	0,98	1,11
A5	2,27	2,00	1,90	2,21	1,21	1,71
A6	1,34	1,26	1,12	1,17	3,06	1,06
A7	1,14	1,02	1,01	1,01	1,02	1,02
Mean ratio (w/m)	1,29	1,20	1,18	1,20	1,16	1,17

CHAPTER 4: EXPOSURE AND CHARACTERIZATION SEISMIC HAZARD

4. Introduction

Environmental degradation, rising social inequality, hyper-urbanization, and the economy are global forces that increase the likelihood of devastation after an earthquake. Social systems in all societies have evolved to alleviate unsafe conditions, reduce the impact of extreme events, and facilitate recovery [41].

This chapter describes the most relevant aspects to accomplish the study of the exposure and characterization of the seismic hazard for unconfined masonry structures (URMM) not greater than 5 stories high.

4.1. Structural modelling

Most of the masonry construction around the world is based on unconfined masonry [17]. Structural typologies using this kind of elements are highly vulnerable [42]. This information has been obtained from the Technical Reports of the World Housing Encyclopedia [43]. This website allows the classification of specific buildings according to the most important construction parameters. The structural behavior of URMM have been used as testbed in this work.

This typology has been and continues to be a dangerous solution to meet the need for affordable housing in the developing world, even in areas with moderate-to-high seismic hazard. In the specific case of Colombia, this type of housing is typical in urban and rural areas, constituting approximately 60% of the existing houses in the country. In there, one can find URMM structures whose number of stories vary from 1 to 5; the typical height of each story is 2.4 m. This type of construction is very prone to damage during an earthquake as it has low seismic performance. In addition, it is worth mentioning that inhabitants involuntarily increase this vulnerability by making inappropriate changes in their homes. These modifications are generally to augment the size of the dwelling. Historically, inhabitants of other countries in the world have also used this typology, with the consequent increase in seismic risk [44].

In earthquake-prone areas, there are many regulations for new construction. In these areas, URMM dwellings are generally forbidden due to its high vulnerability. Notwithstanding, this kind of construction is cheap and, consequently, a significant number of families with limited resource use it. This worsens the general picture of seismic risk in Colombia [17]

Fig. 4-1 presents a schematic of a typical two-story unconfined masonry dwelling. In Colombia, it is not common for this type of housing to exceed five floors.

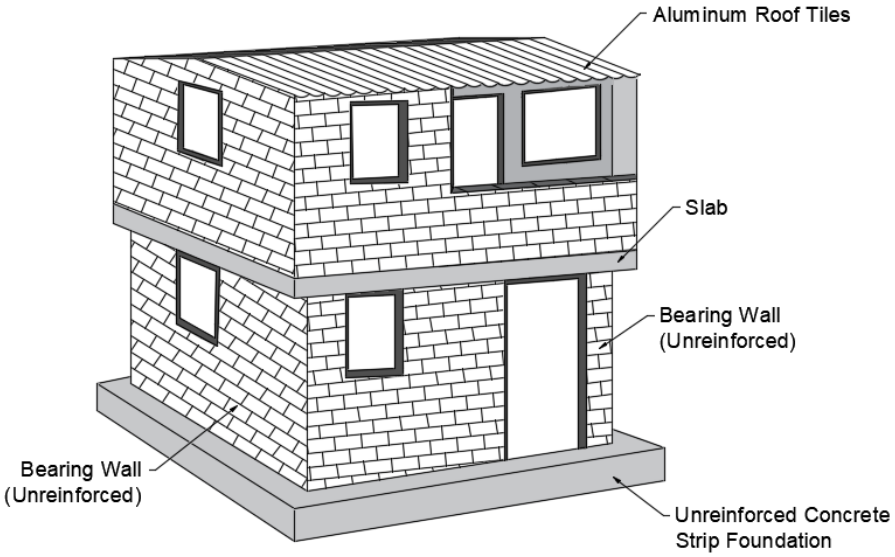

Fig. 4-1. Scheme of a typical unconfined masonry dwelling

4.1.1. Characterization of the exposure

To quantify the main physical characteristics of this typology, the article by Martins & Silva [45], has been used. Due to the probabilistic nature of the dynamic properties of the structures, structural models with random properties were made, varying their period, with respect to the height, following that described in the article by Tarque et al. 2021 [46]. Specifically, it has been assumed that the mean fundamental period of the simulated structures follows a continuous uniform distribution, which allows all the vibration modes of the structure to be considered.

4.1.2. Engineering demand parameters extracted from single degree of freedom systems

To analyse the expected damage of URMM buildings, it is necessary to consider several sources of uncertainty. However, the higher the complexity of the structural model, the higher the computational time to extract reliable information from it. Thus, simplifying the structural model significantly diminishes the computational effort, allowing analysing several building models in a fraction of time.

In this sense, one of the most simplified representations of a building is an SDoF system. This model has been extensively used to estimate the dynamic response of civil structures [45]. It allows calculating time-history responses in an easy way, given a determined fundamental period and damping. However, the response of a single SDoF does not consider neither the stiffness' loss because of plastic damage nor the participation of higher modes. When estimating engineering demand parameters, EDPs, these shortcomings have been addressed by averaging spectral quantities around the fundamental period of the building model. Analogous to this approach, it is proposed to approximate the dynamic response of a building in each direction by averaging the time history response of a set of SDoF systems in the interval ($0.1T_n$, $1.8T_n$). The

response associated with each oscillator has been estimated by means of the dynamic equilibrium equation for SDoF systems:

$$m\ddot{u}_n(t) + c\dot{u}_n(t) + ku_n(t) = -m\ddot{u}_{g,n}(t) \quad \text{Eq. 4-1}$$

where $\ddot{u}_n(t)$, $\dot{u}_n(t)$, and $u_n(t)$ are the spectral acceleration, velocity and displacement time history responses of the SDoF in the *n* direction, respectively; $\ddot{u}_{g,n}(t)$ is the acceleration ground motion; *m*, *c*, and *k* represent the mass, damping, and stiffness of the system, respectively. Thus, the spectral time history response of a building in the *n* direction (*x* or *y*) can be estimated as follows:

$$\ddot{u}_n(t) = \frac{1}{p}\sum_{i=1}^{p} \ddot{u}(t, T_i) \quad \text{Eq. 4-2}$$

$$\dot{u}_n(t) = \frac{1}{p}\sum_{i=1}^{p} \dot{u}(t, T_i) \quad \text{Eq. 4-3}$$

$$u_n(t) = \frac{1}{p}\sum_{i=1}^{p} u(t, T_i) \quad \text{Eq. 4-4}$$

where T_i are the components of a vector of ten periods equally spaced within the interval ($0.1T_x$, $1.8T_x$) for the *x* and ($0.1T_y$, $1.8T_y$) for the *y* directions. In this way, the 3D spectral time history response in terms of acceleration, velocity and displacement of the simulated system has been estimated as follows:

$$\ddot{u}_{(x,y)} = \sqrt{\ddot{u}_x^2 + \ddot{u}_y^2} \quad \text{Eq. 4-5}$$

$$\dot{u}_{(x,y)} = \sqrt{\dot{u}_x^2 + \dot{u}_y^2} \quad \text{Eq. 4-6}$$

$$u_{(x,y)} = \sqrt{u_x^2 + u_y^2} \quad \text{Eq. 4-7}$$

4.1.3. Global drift as EDP

Several EDPs can be extracted from the averaged time-history responses described in the previous section. For instance, the global drift of a structure, *GD*, which is an EDP highly used in estimations of the seismic risk using the capacity spectrum method [47], can be estimated according to the following equation:

$$GD = PF_1 \frac{max\ (u_{(x,y)})}{\mathrm{H}} \quad \text{Eq. 4-8}$$

where PF_1 is the load participation factor [48]; H is the height of the building.

4.2. Seismic hazard characterization

4.2.1. Seismicity in Colombia

Colombia is located within the Pacific Ring of Fire, where most of the world's earthquakes are concentrated. Likewise, Colombia is located on a zone of interaction of three tectonic plates: Caribbean Plate, South American Plate, and Nazca Plate, which makes its seismic hazard much higher compared to other areas of the world.

The greater seismicity is related to the activity of the subduction zone of the Colombian Pacific plate and the different geological faults generated due to the presence of the three plates. Different studies have shown that almost 83% are located within intermediate-high seismic hazard zones [49].

Fig. 4-2 shows the classification of the Colombian territory into three levels of seismic hazard: high in red, medium in yellow, and low in green. These have been determined based on historical and instrumental seismic information provided by the National Seismological Network and the probability of occurrence of different seismic events.

Throughout history there have been seismic events that have caused great damage within the country. The first documented large-magnitude seismic event in Colombia dates from the year 1566. In which the towns of Popayan and Cali suffered great damage, after several mud and tile houses collapsed. After this, the first seismograph was put into operation in 1922, thus founding the Geophysical Institute of the Colombian Andes [50].

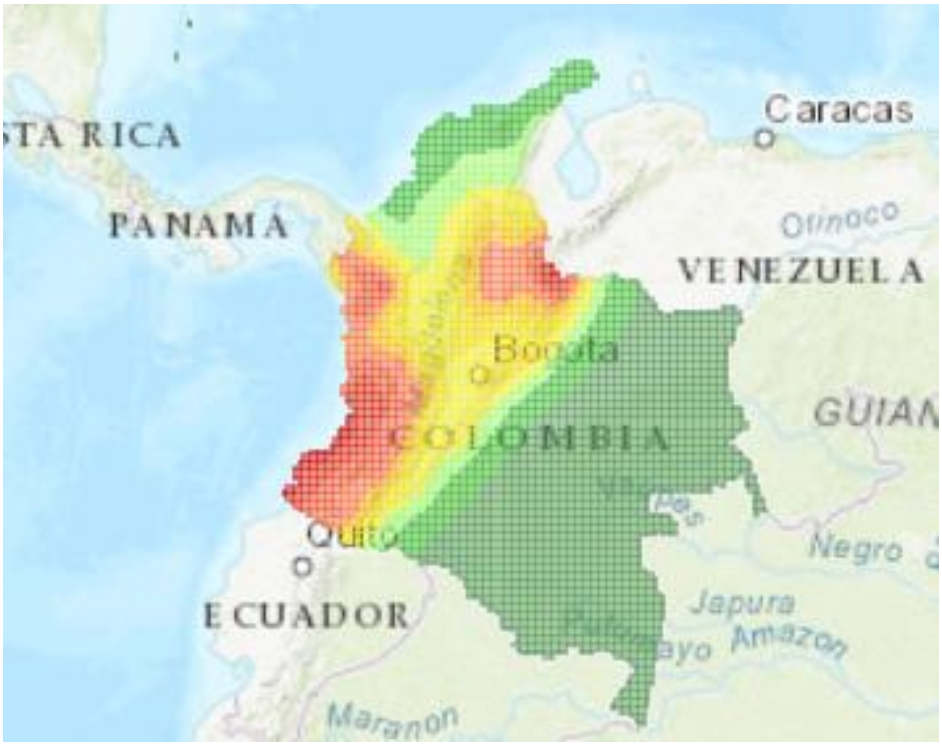

Fig. 4-2. Colombian Seismic Hazard (Image taken from SGC) [13]

Although many of the earthquakes recorded at these dates were attributed to the population where the greatest damage occurred, but not to the epicenter of the event, this provides information of vital importance since it allows generating a trace of the events and their probabilities of occurrence.

For this study, the five regions marked in Fig. 4-3 have been analyzed. Note that these regions have statistical information from the time use survey, [8]. The Central region is the most populated area of the country with an average of 34 million inhabitants; it is also one of the most economically active areas. This region includes the central, eastern, and western mountain ranges that cross the country from southwest to northeast. The total area covered by this region is approximately 2,825,540 km^2, that is, a total of 30% of the territory and a population density of 121.82 inhabitants/km^2. Bogotá, which is the capital of the country and the center of economic movement, located in this region.

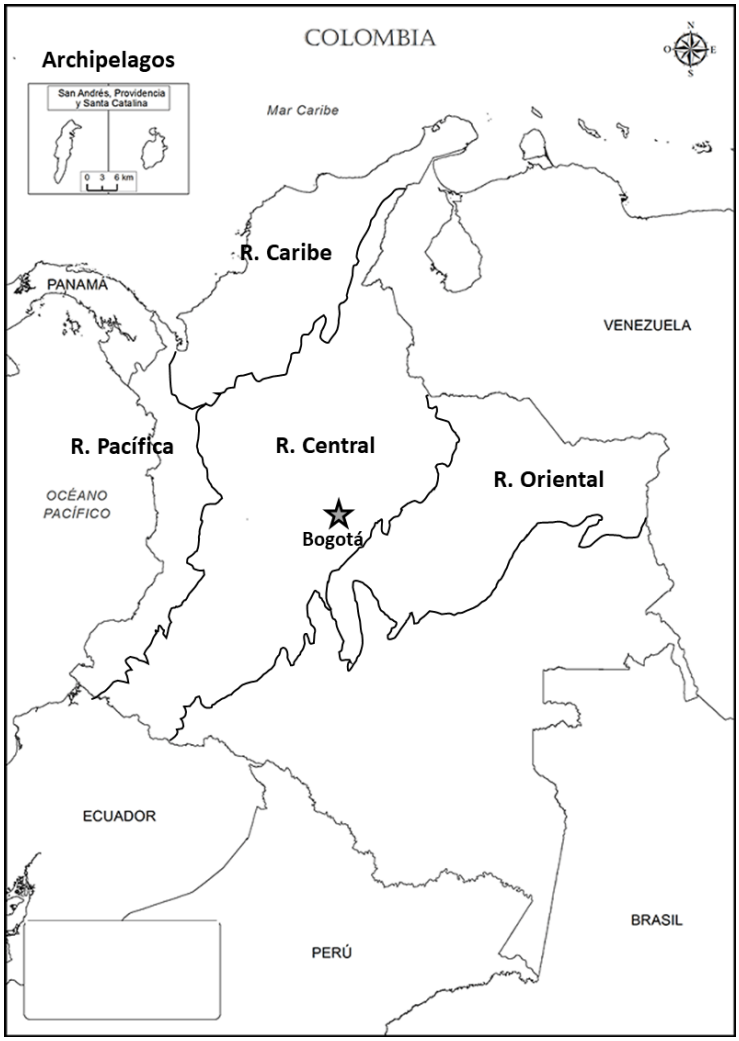

Fig. 4-3. Regions used for the study

Table 4-1. presents a population count for each of the most important population centers in the country.

Table 4-1. Number of inhabitants in Colombia's most important population centers [28]

Department	**Population**
Antioquía	7.621.742
Bogotá	8.674.366
Boyacá	1.272.844
Caldas	1.084.128
Cundinamarca	2.598.245
Huila	1.126.314
Norte de Santander	1.332.335
Quindío	558.934
Risaralda	1.011.283
Santander	2.3403988
Tolima	1.400.203

4.2.2. Definition of seismogenic sources

The geological structure and seismic sources are reflected in the occurrence of earthquakes that are recorded by the seismic network located throughout the territory. The General Seismic Risk Study for Colombia (AIS, 2009) [49] is the basis of the Colombian seismic standard. It includes uniform seismic hazard spectra for each of the capital cities, as well as the design spectrum at rock level for a return period of 475 years. This information has been carried out to select appropriate earthquakes for the seismic design of structures in the country.

The evaluation of the seismic hazard requires the definition of the seismic sources that are influencing the study area. Within the Colombian territory, the AIS 2009 [49] established a total of 38 seismogenic sources, of which 30 correspond to cortical sources, which were defined up to maximum depths of 50 kilometers and minimum depths of 5 kilometers; 8 deep sources are identified, which have depths greater than 50 kilometers.

Fig. 4-4 shows a breakdown of the contribution of the different seismic sources to the hazard of the Colombian territory. For this study, it is intended to analyze different regions of the country. Therefore, sources that generate a greater seismogenic contribution are considered to select ground motion records.

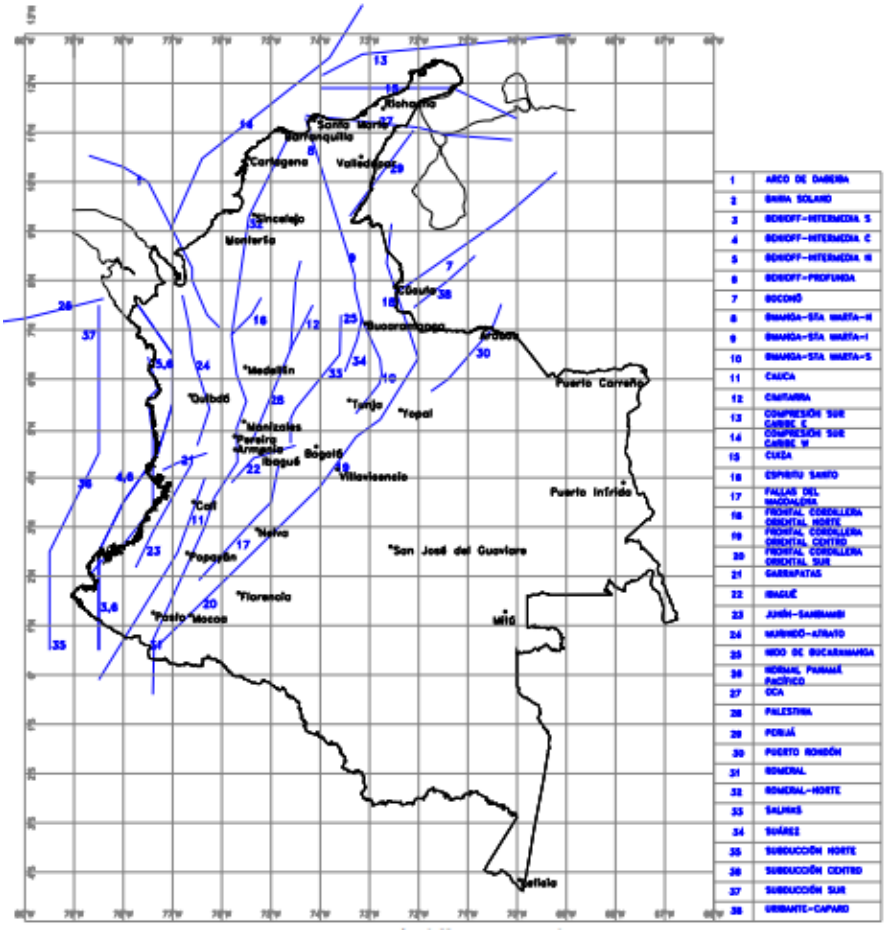

Fig. 4-4. Projection of surface faults within the Colombian territory.[50]

4.2.3. Database of ground motion records

The selection of seismic records should consider how the expected ground motions should be in the study area. Advances in the field of study and technological tools have made it possible to selection procedures, while obtaining more accurate and reliable soil parameters for the estimation of the earthquake hazard.

Followed by this, a compilation has been made of the ground motions recorded between 1993 and 2017, with a magnitude greater than 4.0 Mw. These records have been extracted from the SGC [13]. It has been obtained a total of 648 records that have been used to make better statistics, reduce the uncertainty in the data, and provide a better adjustment to the conditions of the Colombian territory. Ground motion records have been classified into two groups, depending on the conditions in which the signals were recorded. The first one corresponds to signals taken on the bedrock, from which a total of 412 records have been identified. The second group are signals taken on the soil, with a total of 236 records. All the records have a Δt=0.005 sec. It is worth mentioning that only data recorded on bedrock have been used in this study. It seems reasonably

since ground motion recorded on this type of soil tend to affect rigid structures, as the ones analyzed herein.

Upon inspection of these records, it has been observed that some signals are deficient. These conditions do not allow a good representation of the seismic conditions of the area. In addition, it has been necessary to perform a baseline correction to improve the quality of the signals. These requirements have been done through two steps, as indicated in the following.

The first step consisted of developing a code with the MATLAB software, in which the data corresponding to each signal was read, and through an iterative and automatic process, the faulty signals were detected. After this analysis, 194 records on bedrock signals were identified.

The next step consisted mostly of signal processing. A MATLAB code was also developed for performing the baseline correction to each of the signals. In addition, environmental noise and other disturbances that may be interfering with the original signal were identified and corrected.

Fig. 4-5 shows the spectra of the ground motion records selected to carry out this study. In the upper part, in gray lines, the horizontal spectra are shown (E-W, left, and N-S, right) whilst the average of them are shown in red lines. At the bottom, the geometric mean of the horizontal components is presented; average values are also presented in this figure.

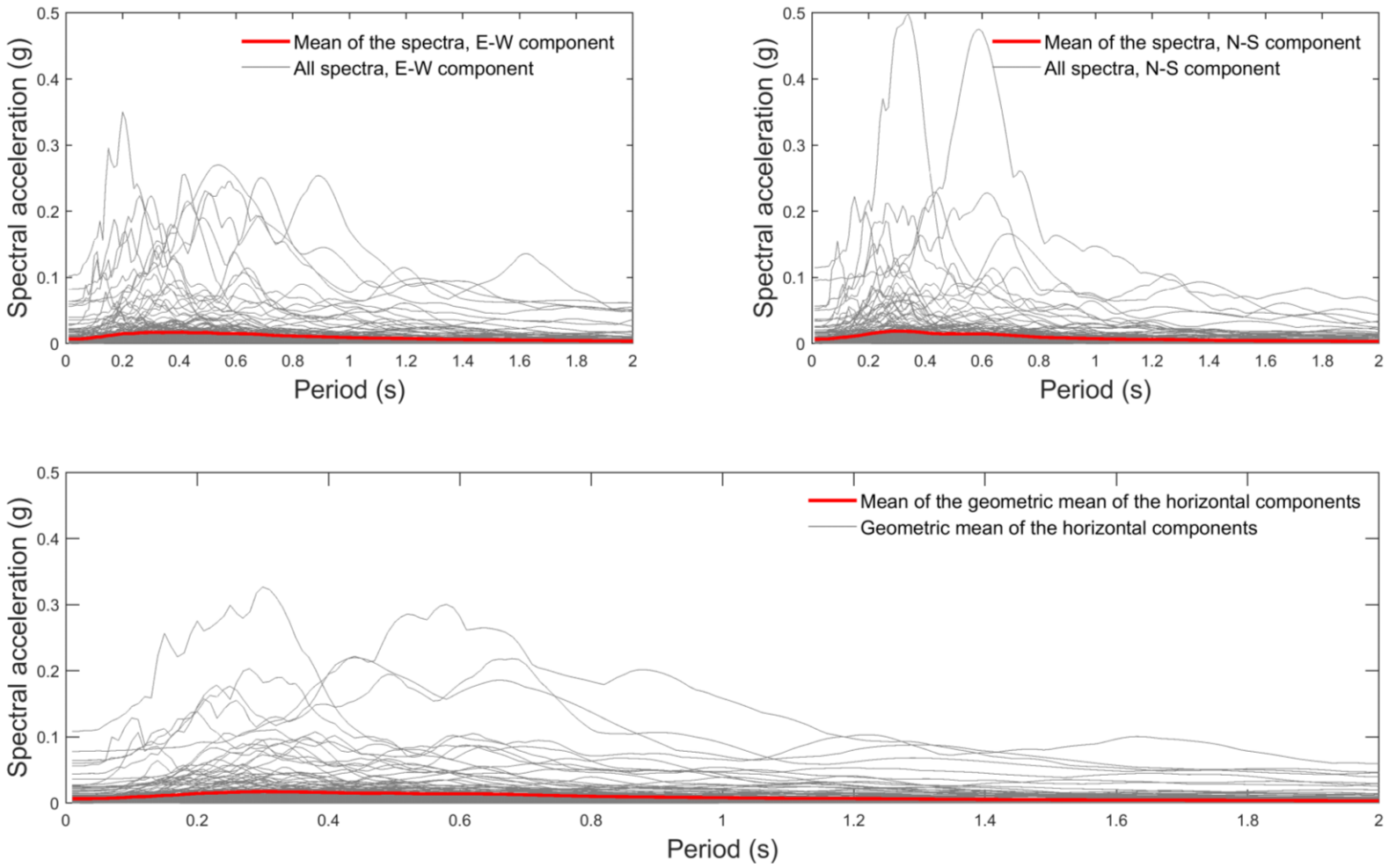

Fig. 4-5. Seismic records selected for the study. Above: Spectra of the horizontal components (Left: E-W component, Right: N-S component). Bottom: Mean and geometric mean of the horizontal components.

4.2.4. Scaling of ground motion

Seismic risk has been quantified in a probabilistic manner. To do so, fragility functions based on the cloud analysis have been derived [18]. This methodology requires obtaining pairs of points that represent the seismic hazard (in terms of intensity measures, IM) and the structural response (engineering demand parameters, EDP). In this research, these points have been obtained through time-history analysis by considering uncertainties in the structural modelling. Consequently, seismic hazard has been characterized by using a probabilistic set of ground motion records.

There are several methodologies to select ground motions from a database [51]. Typically, the goal is to have enough ground motion records that lead the structure to different performance levels. However, the availability of strong ground motion records with high values of the conditioning IM is a common restriction found in current databases. This may trigger excessive scaling that can introduce bias in the structural response [52]. To mitigate these issues when employing cloud analysis, the procedure employed in Vargas-Alzate et al [53] has been used for selecting and scaling (where necessary) ground motion records:

1. Identify the database.
2. Identification of the IM to perform the selection and scaling of the records
3. Calculate the IM identified in the previous step related to each ground motion record
4. Categorize the ground motion records in descending order depending on the calculated IM values
5. Define N_{int} intervals of IM in descending order
6. Define the number of records per interval (N_{rec})
7. The ground motion record ranked as first in the categorization (Step 4) is scaled to fall into the highest interval. If the IM naturally fulfil the interval condition, no scale factor is considered. This step is repeated until having N_{rec} records belonging to the highest interval
8. The last step is repeated to have the desirable number of ground motion records within each interval. The scale factor is calculated so that the IM values are uniformly distributed within the interval

Fig. 4-6 presents a flowchart that summarizes the steps for scaling ground motion records described in this section.

Identifying an optimal IM with the purpose of this thesis (step 2) mainly depends on its efficiency and sufficiency [54]. In this respect, the spectral acceleration at the fundamental period, $Sa(T_1)$, has been one of the most used IMs. However, this IM has been called into question due to its low capacity to explain the non-linear dynamic response of systems [55], or the contribution to the global response of higher modes. Instead, an IM based on the geometric mean of spectral

acceleration values estimated at periods covering both higher and elongated modes of response, Sa_{avg}, has been proven to be more efficiency and sufficient than Sa(T_1) [56–58]. Analogous to this concept, an IM identified as AvSa is considered herein to perform the selection and scaling of the records. Note that AvSa differs from Sa_{avg} since it is calculated using the arithmetic instead of the geometric mean. It is important to note that AvSa is calculated from the geometric mean of the horizontal spectra.

The period range for averaging the spectral ordinates of the IM should be established from the dynamic properties of the entire population of buildings [59]. Accordingly, this range has been set at (0.04-0.71) sec. This period range will be justified in the next section. The intensity levels defining the upper and lower limits of each band (step 5) range from 0.2 to 2.0 g at intervals of 0.2 g (i.e., 10 bands have been defined). Thus, the horizontal components of 190 ground motion records (19 per band) have been obtained from the seismic database. Fig. 4-7 shows the geometric mean spectra of the scaled records.

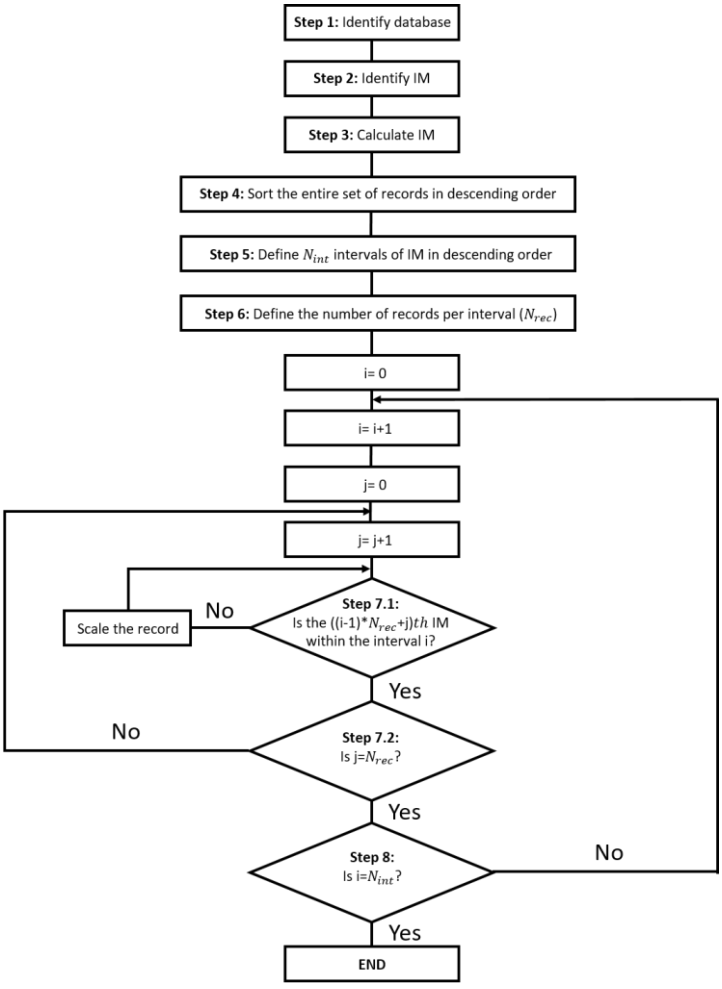

Fig. 4-6. Flowchart illustrating the main steps for selecting and scaling ground motion records [53].

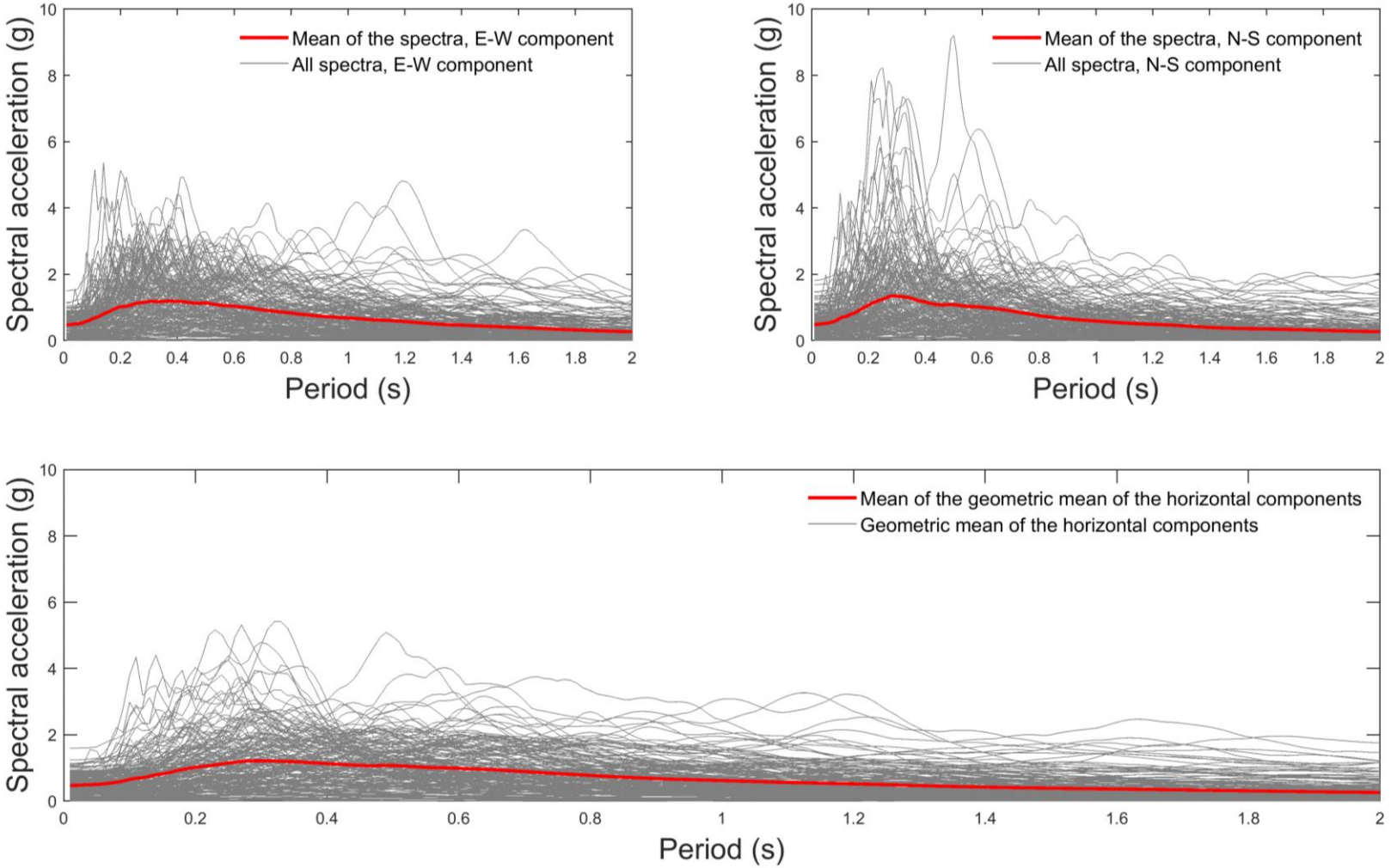

Fig. 4-7. Geometric mean spectra of the selected scaled ground motion records

CHAPTER 5: FRAGILITY ASSESSMENT

5. Introduction

Characterizing fragility is an important step in the probabilistic evaluation of the seismic risk. This chapter describes the development of fragility functions for the URMM housing typology. These functions are derived from the dynamic response of SDoFs subjected to a large number of ground motion records from Colombia (see chapter 4). The resulting fragility functions have been compared with those proposed for this typology in previous research. The derived set of functions have been used to assess human losses due to earthquakes [45].

5.1. Calculation of the EDPs

As commented in previous sections, EDPs are variables extracted from the dynamic response of structures to ground motions; they are used in the design or assessment processes. The most employed EDP is the MIDR. However, other variables such as the maximum roof displacement, maximum global drift (GD) or foundation slip rate can be considered as EDP.

In this research, since the objective is to quantify expected damage, MIDR is used as EDP; this EDP is obtained starting from the MGDR. Thus, the set of IM-EDP pairs is obtained according to the following procedure:

1. Generate a uniform random sample based on a distribution of integers ranging from 1 to 5; this sample represent the number of stories of the simulated models.
2. Estimate the fundamental period of the simulated structure according to Eq. 5-1, which provides the best fit regression analysis to obtain a period of vibration based on the height of an URMM building [16]:

$$T_x = \alpha H^{\beta} \qquad \text{Eq. 5-1}$$

   where α and β are the coefficient providing the best fit curve between a set of data relating height and fundamental period for this typology. In this thesis, coefficients α and β found in Tarque et al. 2012 [46] has been used to consider uncertainties related to the mechanical properties of the materials. That is, α has been assumed to be a Gaussian distribution with mean value equal to 0.09 and a coefficient of variation equal to 0.12; β has been set to 0.75 as in [46].
3. Calculate T_y as a random fraction of T_x. This fraction is obtained as a uniform random sample varying within the interval [0.75 1].
4. Given one T_x-T_y pair, and one ground motion record randomly selected from the entire set, GD is obtained according to the procedure described in sections 4.1.2 and 4.1.3.

5. Because of the relationship between MIDR and GD (see for instance [15,60]), MIDR is estimated as follows: MIDR=1.1*GD.
6. Repeat step 1 to 5 until having ten-thousand IM-EDP pairs.

H has been estimated by assuming that the height of each story is 2.4 m (see Eq. 5-1). Fig. 5-1 shows the relationship between T_x and H according to the procedure described above; the regression fit performed in [46] is also presented in this figure.

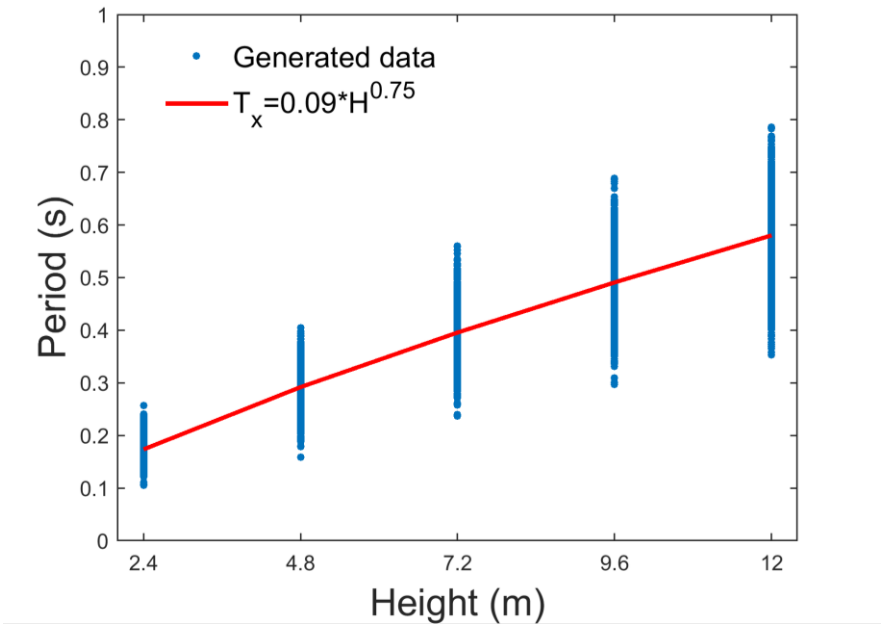

Fig. 5-1 Relationship between T_x and H

As commented in section 4, the aforementioned procedure allows considering not only the fundamental period of the structure but also the participation of higher and lower modes; the latter is intended to take into account the inelastic response of the structure. In addition, for the sake of simplicity, PF_1 (see Eq. 4-8) has been assumed to vary in a linear manner as shown in Fig. 5-2.

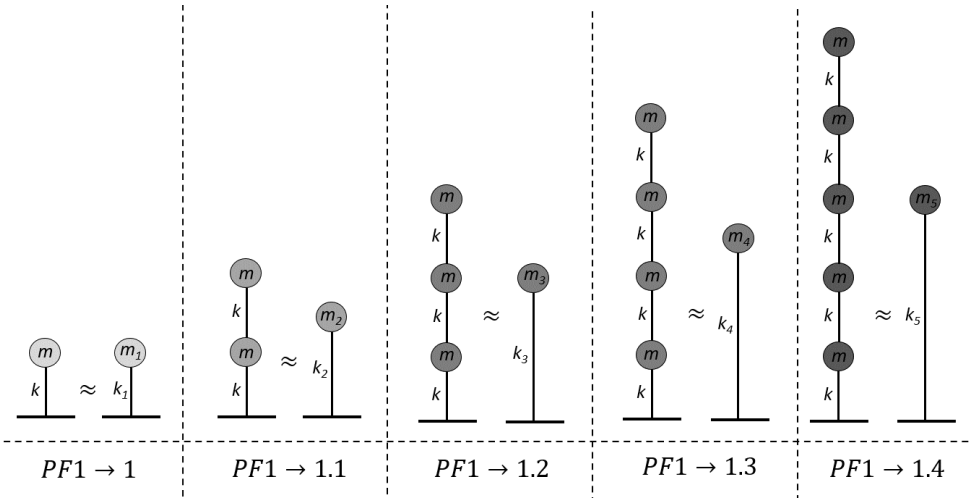

Fig. 5-2. Variation of PF1 depending on the higher of stories

Once building models and ground motion records have been characterized, MIDR can be obtained as described above. Thus, Fig. 5-3 shows the MIDR for the generated models; this figure presents results by considering the entire set of results, and a classification based on the number of stories.

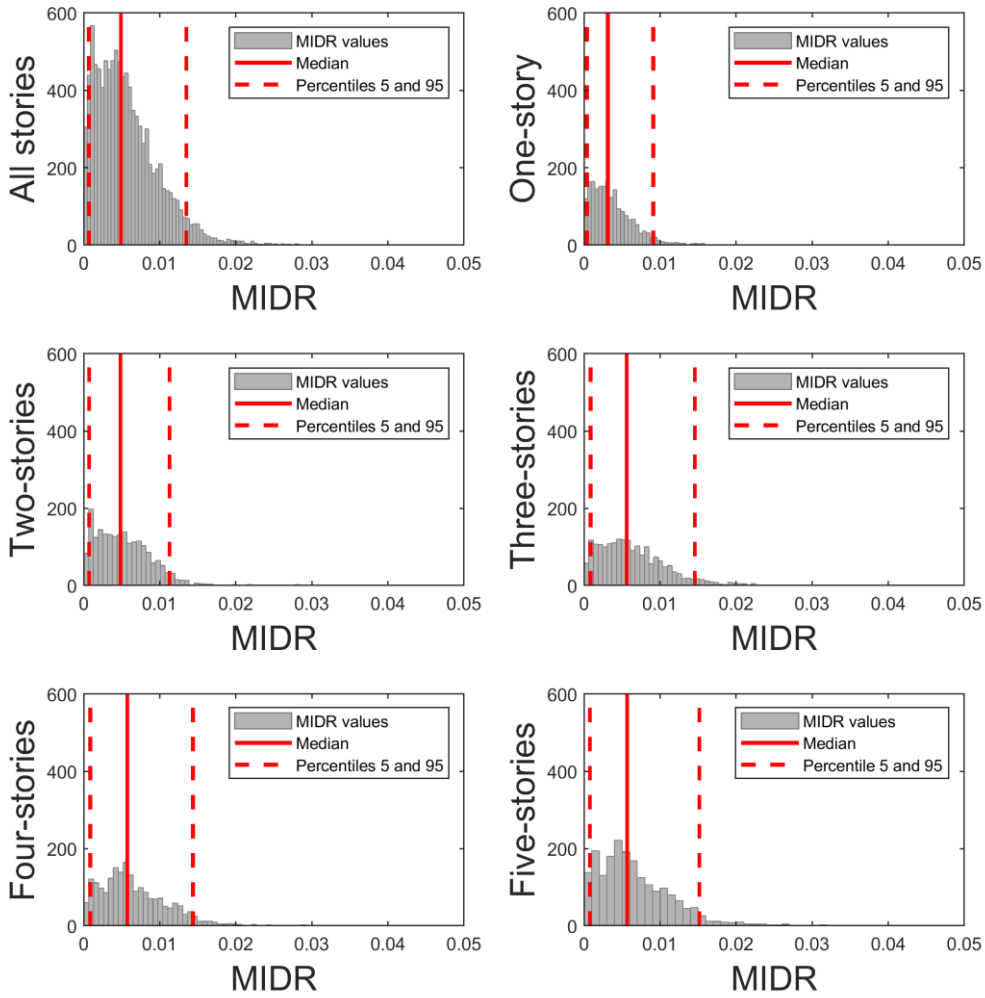

Fig. 5-3. MIDR ratios for all the models

5.2. Intensity measures

IMs can be obtained ranging from the subjective opinion of people who felt the acceleration produced by the ground motion to those calculated from signals recorded by sophisticated devices measuring acceleration amplitudes which humans are not able to detect. In fact, prior to the development of seismological networks worldwide, there was scarce information on the characteristics of ground motion produced by earthquakes. Nowadays, these complex and interactive networks have provided humankind with valuable datasets, allowing to enhance the interpretation of the effect of seismic waves in urban environments. These networks are continuously recording three orthogonal acceleration components at the ground level in several places across the planet. Such records implicitly contain information about the interaction of

physical processes of highly random variability. Basic mathematical background along with proper numerical tools allow extracting from these records variables representing the seismicity of an area. In the context of earthquake engineering, such variables are known as instrumental IMs. Ideally, an IM should contain enough information about the earthquake, so according to it, the structural response can be predicted with confidence [61]. Notice that an IM can depend either on the ground motion properties, or on both the ground motion and structural features [56].

From the statistical point of view, one of the most desirable features that an IM should exhibit is efficiency [54,62,63]. An IM is considered efficient if it reduces the dispersion in the estimated parameter representing the structural response. An IM exhibiting efficiency could potentially reduce the number of structural calculations in estimations of seismic risk at the urban level. In the following, several IMs that have been used in this work are briefly described.

5.2.1. Spectral-Based Intensity Measures

The dynamic response of structures subjected to ground motions has been widely correlated to the peak response of an equivalent SDoF system. The study of this simplified model gives rise not only to the response spectra but also to spectral IMs. It has been recognized that efficient IMs would be defined by response spectral ordinates [15]. Accordingly, response spectral ordinates are extensively used to quantify the seismic hazard at a site. Such ordinates are obtained from the dynamic equilibrium equation for SDoF systems (see Eq. 4-1). IMs from 1 to 6 described in Table 5-1 belong to this category.

5.2.2. Energy-Based Intensity Measures

For both design and assessing the performance of civil structures, the peak response of physical magnitudes like displacement, velocity or acceleration has been widely used. However, several researchers have found that the expected damage of structures can be strongly tied to the amount of energy introduced to the system [64–66]. In this respect, the equivalent velocity spectrum represents the amount of energy introduced to a set of SDoF systems. This energy can be calculated by rewriting Eq. 5-2 in terms of energy. That is, each term of this equation is multiplied by the differential increment of displacement ($\dot{u}_n dt$) and then integrating in the time interval (0, *t*), as follows [67,68]:

$$m\int_0^t \ddot{u}_n \dot{u}_n\, dt + c\int_0^t \dot{u}_n^2\, dt + k\int_0^t u_n \dot{u}_n\, dt = -m\int_0^t \ddot{u}_{g,n}\dot{u}_n\, dt \qquad \text{Eq. 5-2}$$

where $E_{k,n} = m\int_0^t \ddot{u}_n\dot{u}_n\, dt$ is the kinetic energy; $E_{\xi,n} = c\int_0^t \dot{u}_n^2\, dt$ is the energy dissipated by the inherent damping; $E_{a,n} = k\int_0^t u_n\dot{u}_n\, dt$ is the energy absorbed by the system; and $E_{I,n} = -m\int_0^t \ddot{u}_{g,n}\dot{u}_n\, dt$ is the energy introduced into the system by the ground motion. The latter term

is commonly expressed in terms of equivalent velocity, VE, and is normalized with respect to the mass of the structure as follows:

$$VE_n = \sqrt{2E_{I,n}(T_{n,j})} \qquad \text{Eq. 5-3}$$

Calculating VE_n for several elastic oscillators will produce the equivalent velocity spectra. IMs 7 and 8 described in Table 5-1 are obtained from the energy introduced into the system.

5.2.3. IMs Based on Direct Computations of the Ground Motion Record

IMs presented above are based on the spectral response of SDoF systems; this implies that some information related to the structure is included in their estimation. However, several IMs can be obtained from direct computations of the ground motion record. The appeal of this type is that they do not depend on the dynamic properties of the structures. In this way, a generic fragility function could be developed to estimate the seismic performance of buildings with very different structural properties. However, such independency causes a decrease of the efficiency for predicting EDPs, as shown later. IMs from 9 to 18 described in Table 5-1 belong to this category. Note that, when estimating 2D versions of these IMs, they are generally computed as the sum of the IM values calculated for each component of the record.

Table 5-1. Intensity measures description [69]

Intensity Measure	Id	Formula 1D [1]	Formula 2D [2]
Spectral acceleration at $T_{n,j}$	1	$Sa_n(T_{n,j}) = \max(\lvert\ddot{u}_{g,n}(t) + \ddot{u}_n(T_{n,j})\rvert)$	$Sa = \sqrt{Sa_x(T_{x,j}) * Sa_y(T_{y,j})}$
Spectral velocity at $T_{n,j}$	2	$Sv_n(T_{n,j}) = \max(\lvert\dot{u}_n(T_{n,j})\rvert)$	$Sv = \sqrt{Sv_x(T_{x,j}) * Sv_y(T_{y,j})}$
Spectral displacement at $T_{n,j}$	3	$Sd_n(T_{n,j}) = \max(\lvert u_n(T_{n,j})\rvert)$	$Sd = \sqrt{Sd_x(T_{x,j}) * Sd_y(T_{y,j})}$
Average spectral acceleration [3,4]	4	$AvSa_n = \frac{\sum_{i=1}^{n_T} Sa_n(T_i)}{n_T}$	$AvSa = \sqrt{AvSa_x * AvSa_y}$
Average spectral velocity	5	$AvSv_n = \frac{\sum_{i=1}^{n_T} Sv_n(T_i)}{n_T}$	$AvSv = \sqrt{AvSv_x * AvSv_y}$
Average spectral displacement	6	$AvSd_n = \frac{\sum_{i=1}^{n_T} Sd_n(T_i)}{n_T}$	$AvSd = \sqrt{AvSd_x * AvSd_y}$
Equivalent velocity at $T_{n,j}$	7	$VE_n(T_{n,j}) = \sqrt{2E_{I,n}(T_{n,j})}$	$VE = \sqrt{VE_x(T_{x,j}) * VE_y(T_{y,j})}$
Average equivalent velocity	8	$AvVE_n = \frac{\sum_{i=1}^{n_T} VE(T_i)}{n_T}$	$AvVE = \sqrt{AvVE_x * AvVE_y}$
Peak ground acceleration	9	$PGA_n = max(\lvert\ddot{u}_{g,n}(t)\rvert)$	$PGA = \sqrt{PGA_x * PGA_y}$
Peak ground velocity	10	$PGV_n = max(\lvert\dot{u}_{g,n}(t)\rvert)$	$PGV = \sqrt{PGV_x * PGV_y}$
Peak ground displacement	11	$PGD_n = max(\lvert u_{g,n}(t)\rvert)$	$PGD = \sqrt{PGD_x * PGD_y}$

Specific Energy Density [70,71]	12	$SED_n = \int_{t_i}^{t_f} \ddot{u}_{g,n}(t)^2 \, dt$	$SED = SED_x + SED_y$
Arias intensity [72]	13	$I_{A_n} = \frac{\pi}{2\,g} \int_{t_i}^{t_f} \ddot{u}_{g,n}(t)^2 \, dt$	$I_A = I_{A_x} + I_{A_y}$
Characteristic intensity [73]	14	$I_{c_n} = {acc_{RMS}}_n^{1.5} \sqrt{\Delta_n}$	$I_C = I_{C_x} + I_{C_y}$
Root mean of the velocity [5]	15	$vel_{RMS_n} = \sqrt{\frac{1}{\Delta_n} \int_{t_{5\%}}^{t_{95\%}} \dot{u}_{g,n}(t)^2 \, dt}$	$vel_{RMS} = vel_{RMS_x} + vel_{RMS_y}$
Root mean of the acceleration [74]	16	$acc_{RMS_n} = \sqrt{\frac{1}{\Delta_n} \int_{t_{5\%}}^{t_{95\%}} \ddot{u}_{g,n}(t)^2 \, dt}$	$acc_{RMS} = acc_{RMS_x} + acc_{RMS_y}$
Cumulative Absolute Velocity [75]	17	$CAV_n = \int_{t_i}^{t_f} \lvert\ddot{u}_{g,n}(t)\rvert \, dt$	$CAV = CAV_x + CAV_y$
Fajfar intensity [76]	18	$I_{F_n} = PGV_n {\Delta_n}^{\beta}$	$I_F = \sqrt{I_{F_x} * I_{F_y}}$

[1] 1D stands for 1 horizontal dimension. [2] 2D stands for 2 horizontal dimensions. [3] T_i represents a vector of periods around the fundamental period of the structure.[4] n_T is the length of T_i. [5] Δ_n is the significant duration of the record in the *n* direction.

5.3. Efficiency

In this study, IM-EDP relationships have been characterized by means of nonlinear regression analyses in the log-log space. As with linear least squares, nonlinear regression is based on determining the values of the parameters that minimize the sum of the squares of the residuals. In this sense, the following general linear least-square model allows several types of regression:

$$y = \sum_{i=1}^{m+1} \alpha_{i-1} z_{i-1} + \varepsilon \qquad \text{Eq. 5-4}$$

where $\alpha_0, \alpha_1, \ldots \alpha_m$ are the coefficients providing the best fit between model and data; $z_0, z_1, \ldots z_m$ are basic functions; ε represents the residuals. It can easily be seen how polynomial regression falls within this model. That is, $z_0 = 1$, $z_1 = x$, $\ldots z_m = x^m$ [77]. Substituting in Eq. 5-4 $y = \ln EDP$ and $z_{i-1} = (\ln IM)^{i-1}$, the linear least-square model using polynomial functions can be used to extract statistical information from IM-EDP pairs according to the following equation (Eq. 5-5):

$$\ln EDP = \sum_{i=1}^{m+1} \alpha_{i-1} (\ln IM)^{i-1} + \varepsilon \qquad \text{Eq. 5-5}$$

For *m=2*, Eq. 5-5 adopts the following quadratic form:

$$\ln EDP = \alpha_0 + \alpha_1 \ln(IM) + \alpha_2 \ln(IM)^2 + \varepsilon \qquad \text{Eq. 5-6}$$

where α_0, α_1 and α_2 are scalars maximizing the coefficient of determination, R^2, between IM-EDP pairs. This variable is generally used to quantify efficiency when analyzing IM-EDP pairs (see for instance [78]). For a perfect fit, R^2=1, signifying that the quadratic function explains 100% of the data variability. R^2 is used herein to provide an estimation of the variability when analyzing relationships involving IM-EDP pairs. That is, the higher R^2 the lower the variability when predicting some EDP given an IM. Consequently, the IM providing the highest R^2 will be the most efficient IM, in the sense that it allows reducing the variability in seismic risk estimations. Further information regarding the development and implementation of this type of polynomial models in the log-log space can be found in Chapra (2017) [77].

Fig. 5-4 shows the relationship between the set of IMs and the MIDR. This figure presents results by considering all the simulated structures. That is, the results from URMM models of one- to five-stories have been analyzed simultaneously. Fig. 5-4 shows that the three most efficient IMs are AvVE, AvSa and AvSv. This confirms that averaged spectral values tend to be more correlated with the simulated response of structures.

At this point, it is important to note that there is an efficiency loss for several IMs when combining results from models representing dwellings with different numbers of stories. It means that these IMs are not steadfast (Vargas-Alzate et al. 2022 [14]). In brief, steadfastness is related to stability of efficiency for predicting the behaviour of building populations with increasing diversity. In other words, the efficiency does not significantly decrease when combining results of models with different geometrical features (e.g. number of stories). To check the amount of efficiency loss, ANNEX A presents the clouds of IM-EDP points after classifying results by the number of stories. AvSd becomes the most efficient IM for all the cases. However, for the sake of simplicity, in order to derive fragility functions, it has been opted to use IMs exhibiting steadfastness.

It is worth mentioning that although AvVE is more efficient than AvSa, in Colombia there are Uniform Hazard Maps only in terms of spectral acceleration. Therefore, for the sake of simplicity, a generic fragility function based on AvSa will be used to: i) develop fragility functions for several damage thresholds; and ii) estimate the number of affected people according to (Hazus 99 [19]).

5.4. Derivation of fragility functions

From a set of IM-EDP pairs, one can derive fragility functions according to the so-called ‘cloud analysis’ approach [18]. This methodology requires to calculate the best fit curve between a set of IM and EDP realizations in the log-log space. The resultant curve is used to estimate the mean value of a parametric statistical distribution, given an IM value. The variability of this parametric distribution ($S_{y/x}$) is estimated as the standard deviation of the IM-EDP residuals with respect to the fitted curve. In this way, the probability of exceeding a certain damage threshold can be

calculated. These thresholds are realizations of the engineering demand parameter under consideration, EDP_C.

In this study, four damage states are considered, ranging from slight to complete damage; they are calculated by means of Eq. 5-7 to Eq. 5-10:

$$DS1 = 0.75\ \mathrm{Sd}_y \quad \text{Eq. 5-7}$$

$$DS2 = 0.50\ \mathrm{Sd}_y + 0.33\ \mathrm{Sd}_u \quad \text{Eq. 5-8}$$

$$DS3 = 0.25\ \mathrm{Sd}_y + 0.67\ \mathrm{Sd}_u \quad \text{Eq. 5-9}$$

$$DS4 = \mathrm{Sd}_u \quad \text{Eq. 5-10}$$

In these equations, Sd_y =0.12% (yielding displacement) and $\mathrm{Sd}_u = 0.55\%$ (ultimate displacement); these limits are obtained from [46,79–81] Table 5-2 shows the calculated values according to Eq. 5-7 to Eq. 5-10.

Table 5-2. Damage threshold for URMM [45]

	Slight (DS1)	**Moderate (DS2)**	**Severe (DS3)**	**Complete (DS4)**
Damage threshold	0.0009	0.0018	0.0039	0.0055

In this manner, fragility functions presented in Fig. 5-5 have been derived by considering the damage thresholds shown in Table 5-2.

.

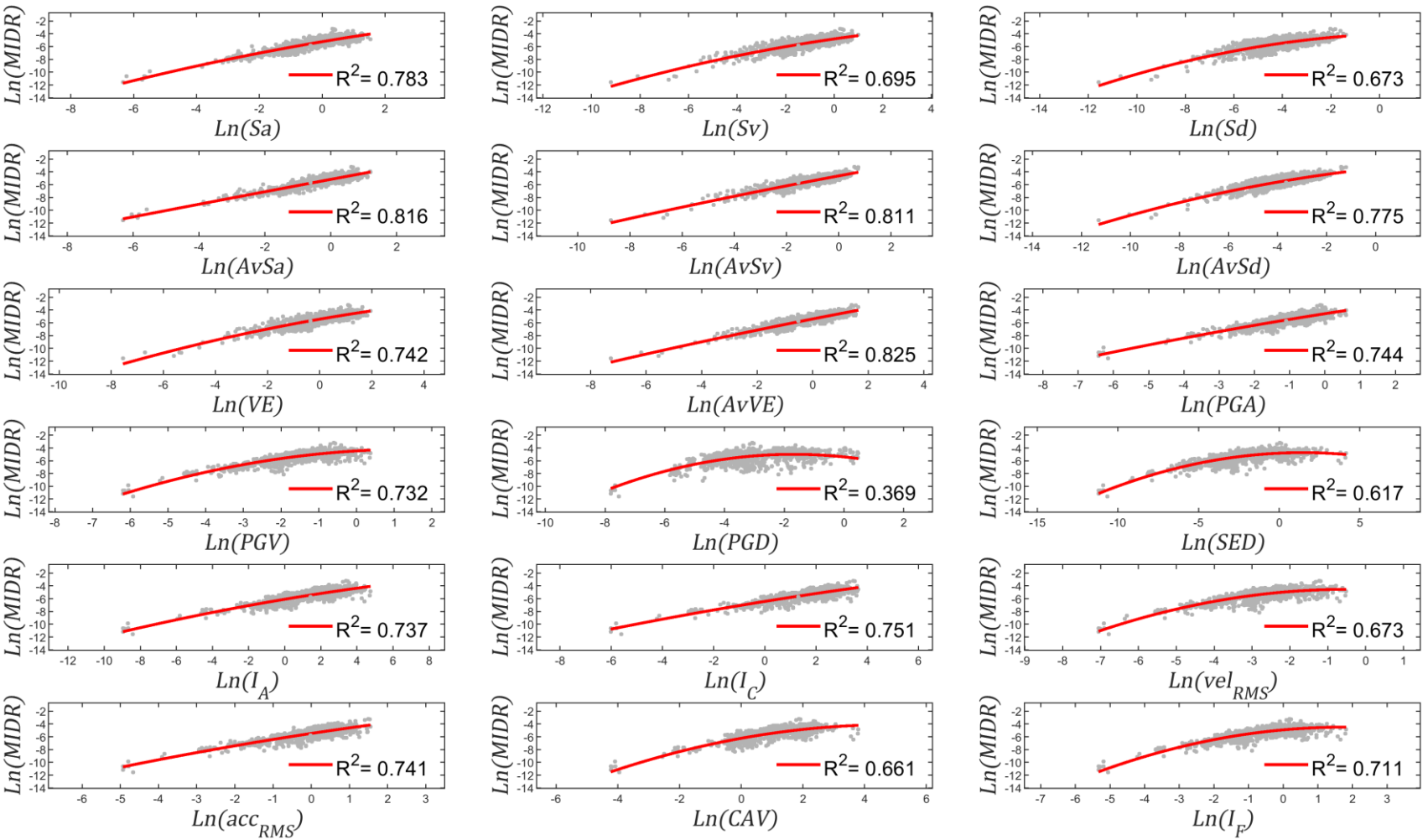

Fig. 5-4. Ten-thousand IM-EDP pairs from URMM building models of one- to five-stories

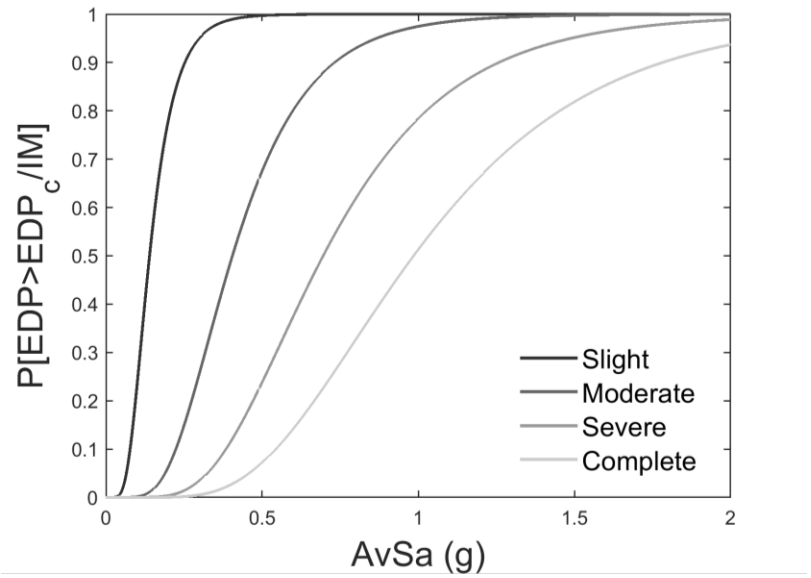

Fig. 5-5. Fragility functions for URMM buildings

5.5. Earthquake scenarios

To estimate expected risk by considering a gender classification, the first step consists in estimating the expected demand (in terms of IMs) for each of the analysed regions (see Fig. 4-3). To do so, the Uniform Hazard Spectra (UHS) of the main cities are extracted from the Colombian Seismic Hazard Consultation System [13]. Fig. 5-6 presents a snapshot extracted from this website.

Fig. 5-6. Colombian Seismic Hazard Map Viewer [13]

Hence, UHS spectra for return periods equal to 31, 225, 475, 975 and 2475 years are obtained; Fig. 5-7 presents these spectra. Based on these spectral functions, AvSa has been calculated for each region (see Table 5-3). Because of the probabilistic approach adopted in this study, there is not a single structural model but a group of them which, in addition, have highly variable fundamental periods (see Fig. 5-1). Therefore, the period range for averaging the spectral ordinates is established from the dynamic properties of the entire population of buildings. The period range for calculating this IM has been (0.04-0.7) s.

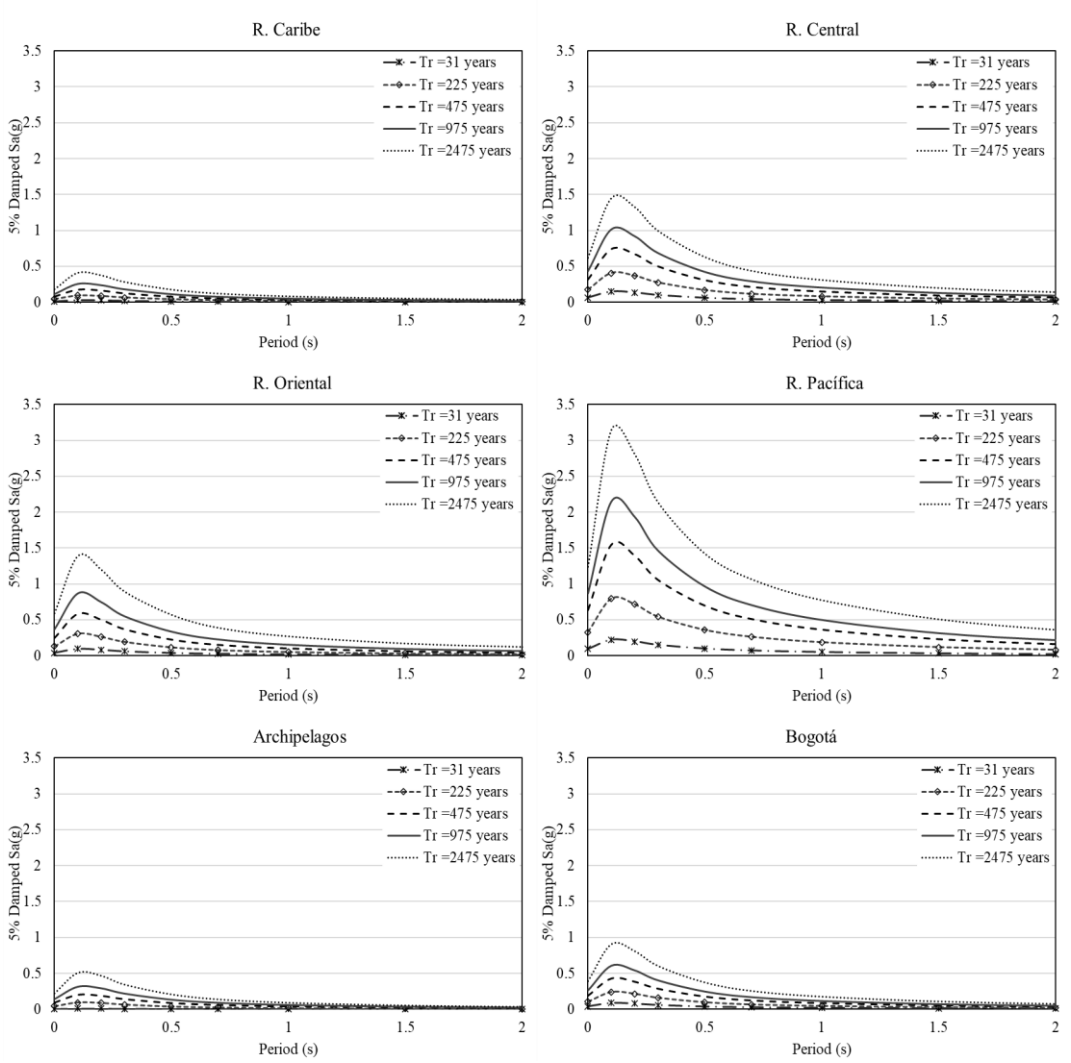

Fig. 5-7. Uniform hazard spectrum, UHS, for return periods equal to 31, 225, 475, 975 and 2475 years for each region

It can be seen from Table 5-3 that the Pacific region exhibits the highest AvSa values; their acceleration values are almost double compared to the other regions. This is due to the fact that this region is closer to the Pacific subduction zone. In contrast to this, regions located at the opposite extreme (towards the Caribbean Sea) drastically decrease their acceleration values, as is the case of the archipelagos, where the maximum acceleration values do not exceed 0.5 g at any return period.

Table 5-3. AvSa over a period range of [0.04 - 0.7] s

Return Period	AvSa (g)					
	R. Caribe	R. Central	R. Oriental	R. Pacifica	Archipelagos	Bogotá
Tr =31 yrs	0.0206	0.1086	0.0671	0.1611	0.0067	0.0637
Tr =225 yrs	0.0691	0.2938	0.2156	0.5816	0.0683	0.1714
Tr =475 yrs	0.1316	0.5326	0.4070	1.1235	0.1478	0.3103
Tr =975 yrs	0.1912	0.7311	0.6092	1.5642	0.2275	0.4379
Tr =2475 yrs	0.2981	1.0572	0.9850	2.2794	0.3676	0.6547

5.6. Injury level estimation

The methodology presented in Hazus 99 to estimate injuries has been applied in this research [19]. Specifically, the indoor casualty rates (see Tables 13.3-8 of Hazus 99) has been used to estimate the probability of suffering a certain injury severity level. This methodology requires the estimation of the probability of occurrence of each damage state given an intensity level (Intensity level values can be extracted from Table 5-3). Then, the probability of occurrence of each damage state have been calculated from the fragility functions presented in Fig. 5-5. In this way, the probability of people suffering an injury level i, P_{Li}, has been estimated based on the values provided in Tables 13.3-8 of Hazus 99. Accordingly, four injury levels have been considered:

Table 5-4. Injury Classification Scale [19] (Extracted from Hazuz 99)

Injury Severity Level	Injury Description
Severity 1	Injuries requiring basic medical aid that could be administered by paraprofessionals. These types of injuries would require bandages or observation. Some examples are: a sprain, a severe cut requiring stitches, a minor burn (first degree or second degree on a small part of the body), or a bump on the head without loss of consciousness. Injuries of lesser severity that could be self-treated are not estimated by HAZUS.
Severity 2	Injuries requiring a greater degree of medical care and use of medical technology such as x-rays or surgery, but not expected to progress to a life-threatening status. Some examples are third degree burns or second degree burns over large parts of the body, a bump on the head that causes loss of consciousness, fractured bone, dehydration, or exposure.
Severity 3	Injuries that pose an immediate life-threatening condition if not treated adequately and expeditiously. Some examples are: uncontrolled bleeding, punctured organ, other internal injuries, or crush syndrome.
Severity 4	Instantaneously killed or mortally injured

The next step consists in estimating the number of affected people based on the following equation:

$$N_{ILi} = P_{Li} * Pg * Ph * N_p \qquad \text{Eq. 5-11}$$

where N_{ILi} represents the number of affected people with an injury level i; P_{Li} is the probability of suffering injury level i; Pg is the probability of being women or men; Ph represents the probability of being at home (Table 3-1); and N_p is the number of people considered in the analysis. For the sake of simplicity, this number has been assumed as 100 000. Regarding Pg, the last cadastral census carried out in Colombia indicated that the percentage of women is 51.2% and that of men 48.8%. Based on Eq. 5-11, the number of affected people discretized by region, and for return periods equal to 475 and 2475 years is presented in Table 5-5 (for women) and Table 5-6 (for men).

It is observed in all regions that the number of affected women is higher than that of men, especially in the Caribbean region, where the difference between affected women and men exceeds 35% for a Tr=2475 years. It should be noted that, in this region and the Archipelagos, for damage levels 3 and 4, and for return periods equal to 475 years, the number of affected people is insignificant, therefore, they are not presented in this study.

The data from Bogotá and Archipelagos represent the lowest percentages of difference (22%), similar for the two return periods analyzed. For the Pacific region, which presents the highest hazard, the difference observed is around 25%. Note that for some regions, the number of people who may be affected by a seismic catastrophe is very high and may amount to an approximate total of 10,000 and 15,000 victims for return periods equal to 475 and 2475 years, respectively. It is worth mentioning that the total amount of affected people will depend on the number of citizens belonging to each region. In other words, a greater number of wounded is expected for the central region, since this area is the one with the largest population in the country.

Table 5-5. Number of women affected, disaggregated by level of injury, region and return period. Data presented is for every 100 000 people

Number of women affected												
Level of injury	**R. Caribe**		**R. Central**		**R. Oriental**		**R. Pacifica**		**Archipelagos**		**Bogotá**	
	Tr=475 yrs	Tr=2475 yrs	Tr=475 yrs	Tr=2475 yrs	Tr=475 yrs	Tr=2475 yrs	Tr=475 yrs	Tr=2475 yrs	Tr=475 yrs	Tr=2475 yrs	Tr=475 yrs	Tr=2475 yrs
N_{IL1}	10.9	105	808.3	3721.2	324.9	3363	3793.7	5671.1	12.6	199.7	109.3	1330.6
N_{IL2}	1.3	51	277.6	1177	130.2	1061.8	1202.4	1833.4	2.3	86	52.2	429.9
N_{IL3}	N/A	1.8	30.7	184.2	9.5	164.3	189.7	298.7	N/A	5.1	2	57
N_{IL4}	N/A	3.4	60.4	364.1	18.6	324.6	375	590.7	N/A	9.9	3.9	112.4
Total	12.2	161.2	1177	5446.5	483.2	4913.7	5560.8	8393.9	14.9	300.7	167.4	1929.9

Table 5-6. Number of men affected, disaggregated by level of injury, region and return period. Data presented is for every 100 000 people

Number of men affected												
Level of injury	**R. Caribe**		**R. Central**		**R. Oriental**		**R. Pacifica**		**Archipelagos**		**Bogotá**	
	Tr=475 yrs	Tr=2475 yrs	Tr=475 yrs	Tr=2475 yrs	Tr=475 yrs	Tr=2475 yrs	Tr=475 yrs	Tr=2475 yrs	Tr=475 yrs	Tr=2475 yrs	Tr=475 yrs	Tr=2475 yrs
N_{IL1}	8.1	77.7	644.2	2965.5	262	2711.6	3023.3	4519.5	10.3	163.5	89	1084.2
N_{IL2}	1	37.7	221.2	938	105	856.1	958.2	1461.1	1.9	70.4	42.5	350.3
N_{IL3}	N/A	1.3	24.5	146.8	7.7	132.4	151.2	238	N/A	4.2	1.7	46.4
N_{IL4}	N/A	2.5	48.1	290.2	15	261.7	298.9	470.8	N/A	8.1	3.2	91.6
Total	9.1	119.2	938	4340.5	389.7	3961.8	4431.6	6689.4	12.2	246.2	136.4	1572.5

5.7. Armenia's Earthquake

On January 25, 1999 at 13:19 pm there was a strong earthquake of magnitude 6.3 Mw, which released a significant amount of energy that seriously affected the infrastructure of the area and compromised the safety of the surrounding inhabitants. According to the DANE's report on this event, [7] it was quantified a total of 1,185 casualties, 8,536 injured, 35,972 houses were destroyed or uninhabitable (the vast majority of them were URMM buildings) and 4,467 houses were partially affected. Out of the total number of casualties during the catastrophe, 78% were concentrated within the city of Armenia.

The most intense ground motion was recorded at the Cordoba station; Fig. 5-8 shows the acceleration spectra of the E-W and N-S components of this record.

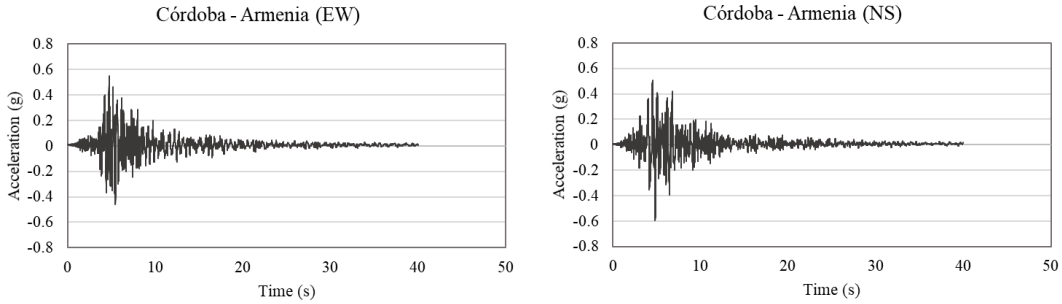

Fig. 5-8. Horizontal ground motion recorded at the Cordoba station

From these records, it is possible to extract AvSa values. To do so, it is necessary to obtain the spectra for both components. Hence, in the upper part of Fig. 5-9, the acceleration spectra are presented for each of the horizontal components (E-W and N-S); in the lowest part of this figure, the geometric mean spectrum is presented. From this spectrum, AvSa= 1.09 g (the period intervals between 0.04 and 0.7 sec have been used to estimate this IM).

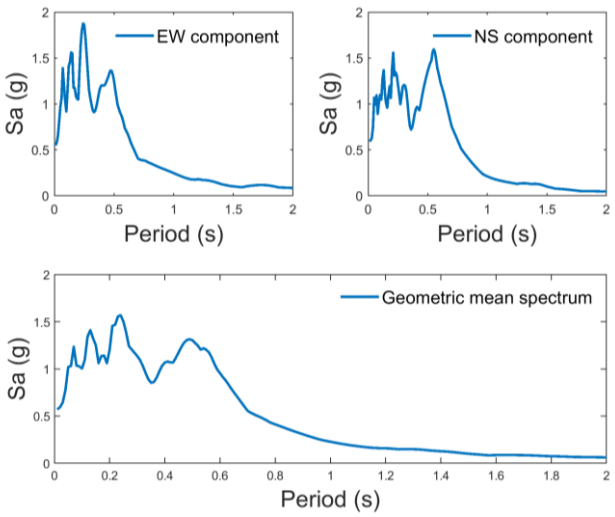

Fig. 5-9. Spectral acceleration for the Armenian earthquake. Above: Spectral acceleration of the horizontal components. Bottom: Geometric mean of horizontal components.

This section is dedicated to comparing the number of affected people observed in the Armenian catastrophe with those simulated with the previous approach, allowing to determine if the developed model adjusts to the real conditions of the affected area.

Following the above, the data on the population affected by this earthquake are taken from the DANE report [7], which states that during the emergency, a total of 921 casualties and 383 disappeared were reported for the city of Armenia. In the case of men, a total of 445 casualties and 128 disappearances were reported, whilst on the women's side these numbers were 476 casualties and 255 disappearances. That is, for injury level 4, the number of men was 573 and women 731. These data confirm the imbalance in the expected risk by gender.

The next step is to estimate the number affected people suffering an injury level 4, based on the methodology presented in this research. To do so, the AvSa value extracted from the spectra of the ground motion record presented in Fig. 5-8 is obtained (i.e. AvSa=1.09 g). Based on this value, the probability of occurrence of each damage state is estimated from the fragility functions presented in Fig. 5-5.

Table 5-7 Probability of occurrence of each damage state given that AvSa=1.09 g

	Slight	**Moderate**	**Severe**	**Complete**
Probability of occurrence	0.0163	0.1495	0.2471	0.5870

Based on these probabilities, and by considering that 214 388 were the number of inhabitants in the city of Armenia for that time, the number of men suffering injury level 4 is equal to 650 (573 were reported), whilst on the women's side, this number is 816.5 (731 were reported). These values have been obtained by applying Eq. 5-11, and by considering the use of time for this region (see Table 3-1). Although these numbers are not the same as those observed in the catastrophe, they provide a satisfactory estimate not only in terms of the number of people affected, but also the distribution by gender.

CONCLUSIONS

This study has presented a quantification by gender of the risk of injury in the event of earthquake catastrophes in Colombia. The main objective has been to provide a better visualization of the role of women within the Colombian household and how the fact that they assume most of the unpaid work increases their vulnerability to being affected in the event of the collapse of their homes.

In line with the above, the results of the Colombian time-use survey [8] revealed that Colombian women spend, on average, 20% more time at home than men because they are mainly in charge of the household chores. This time imbalance is in line with that presented on the Sustainable Development Goals website [1], where it is confirmed that after studies carried out between 2001 and 2019 in 90 countries and areas, women spend an average of 2.5 times more time inside their homes because they oversee unpaid household activities.

For this study, a highly vulnerable structural typology (URMM) has been studied. Note that despite the high vulnerability of this typology, it is present in most countries in the world. In fact, several global earthquake-related catastrophes may be associated with the use of this type of vulnerable housing. In this regard, it is worth mentioning that sometimes the inhabitants involuntarily increase the vulnerability of their home by making inappropriate modifications. Therefore, it is very important to easily communicate the possible consequences of these actions to the non-specialized community. It is also a means for politicians and decision-makers to propose new laws aimed at improving the resilience of civil infrastructure. In general, it is of utmost importance to mitigate the seismic risk associated with vulnerable typologies, otherwise the achievement of several sustainable development goals may be compromised [1].

A fragility model based on the contribution of several SDoF systems, whose vibration period is around the expected one for this typology, has been developed in this research. To do so, a set of ground motion recorded in Colombia has been used to represent seismic hazard. The cloud analysis has been employed to derive the fragility functions [18]. Based on these functions, the expected risk in terms of injuries has been estimated. The Hazuz methodology to estimate injuries has been used in this research [19]. Five regions of Colombia have been selected for this investigation. In each of the regions, a notable difference is observed between the number of men and women who may be affected, thus verifying how gender inequality is reflected after a seismic catastrophe.

After analysing data from a catastrophic event that occurred in a Colombian city, Armenia, it has been possible to verify the tendency of women to be more affected than men [7] due to a seismic catastrophe. This event has also been used to verify the reliability of the developed model. This validation is of paramount importance since it allows the development of a reliable and

comprehensive tool for decision-making in terms of seismic risk mitigation, not to mention that it can be used to visualize the risk to which women are exposed by staying longer inside vulnerable homes.

It is worth mentioning that the imbalance in risk could be explained by the fact that more women than men lived in the affected places. However, this is also a consequence of gender inequality, as more women than men live in vulnerable places.

In terms of future research activities, it will be of interest to recalculate fragility functions by disaggregation based on the number of stories. It is expected that results based on this classification will be more reliable. In addition, it has been observed that IMs based on velocity an energy are more efficient than that based on acceleration (at least when the entire set of models is simultaneously considered). However, to develop results based on these quantities, new UHS maps should be derived for the analysed area.

It is considered that all the objectives proposed for this thesis have been satisfactorily achieved, however, this research does not intend to stop here. This study seeks to encourage the different countries to develop and implement this type of study within their territories, thus giving a better visualization of the current situation, allowing the application of adequate mitigation measures, to protect not only the lives of women, but that of the entire vulnerable population. Nonetheless, according to the results presented in this study, increasing the performance of vulnerable typologies can be a direct action to mitigate gender inequalities, especially in low-income regions. In addition, this research seeks to raise awareness about the importance of developing better social strategies for the empowerment of women, not only due to the injustice related to gender inequality, but also as a measure of protection for themselves.

REFERENCE

[1] United Nations, Sustainable Development, (n.d.). https://sdgs.un.org/ (accessed November 28, 2021).

[2] A. Coburn, R. Spence, Earthquake Protection - Andrew Coburn, Robin Spence - Google Libros, John Wiley & Sons. (2003).

[3] F. Denton, Climate change vulnerability, impacts, and adaptation: Why does gender matter?, Https://Doi.Org/10.1080/13552070215903. 10 (2010) 10–20. https://doi.org/10.1080/13552070215903.

[4] E. Neumayer, T. Plümper, The Gendered Nature of Natural Disasters: The Impact of Catastrophic Events on the Gender Gap in Life Expectancy, 1981–2002, Annals of the Association of American Geographers. 97 (2007) 551–566. https://doi.org/10.1111/j.1467-8306.2007.00563.x.

[5] S. Walia, A. Rathi, Why women are more at risk than men in earthquake-ravaged Nepal — Quartz India, (2015). https://qz.com/india/392867/ (accessed November 26, 2021).

[6] E. Frankenberg, T. Gillespie, S. Preston, B. Sikoki, D. Thomas, MORTALITY, THE FAMILY AND THE INDIAN OCEAN TSUNAMI, Econ J (London). 121 (2011) F162. https://doi.org/10.1111/J.1468-0297.2011.02446.X.

[7] DANE, Dimensión social y económica de los efectos del terremoto del eje cafetero. Diagnóstico para la reconstrucción, Santafé de Bogotá, 1999.

[8] DANE, Encuesta Nacional de Uso del Tiempo-- ENUT, (2017). https://www.dane.gov.co/index.php/estadisticas-por-tema/demografia-y-poblacion/52-espanol/noticias/noticias/2648-enut-2012-2013 (accessed November 28, 2021).

[9] E. Studer, The South Asia Women's Resilience Index Examining the role of women in preparing for and recovering from disasters, Poverty Wellbeing. (2014).

[10] S. Bhalotra, C. Sanhueza, Y. Wu, Long-term economic consequences of the 1960 Chile earthquake, (2011).

[11] Sistema Nacional de Prevención y Atención de Desastres (SNPAD), Colombia: Integrating disaster risk reduction at the local level, 2005.

[12] L. Tanner, D. Markek, C. Komuhangi, Women's Leadership in Disaster Preparedness, (2018).

[13] Colombian geological survey (SGC), Sistema de Consulta de la Amenaza Sísmica de Colombia, (n.d.). https://amenazasismica.sgc.gov.co/ (accessed November 28, 2021).

[14] Y.F. Vargas-Alzate, J.E. Hurtado, L.G. Pujades, New insights into the relationship between seismic intensity measures and nonlinear structural response, Bulletin of Earthquake Engineering. 20 (2022) 2329–2365. https://doi.org/10.1007/s10518-021-01283-x.

[15] Y.F. Vargas Alzate, L. Pujades Beneit, J.R. González Drigo, R.E. Alva Bañuelos, L. Pinzón Ureña, On the equal displacement aproximation for mid-rise reinforced concrete buildings, in: International Conference on Computational Methods in Structural Dynamics and Earthquake Engineering, Institute of Structural Analysis and Antiseismic Research School of Civil Engineering. National Technical University of Athens (NTUA), Crete, Greece, 2019: pp. 5490–5502.

[16] R.K. Goel, A.K. Chopra, Period Formulas for Moment-Resisting Frame Buildings, Journal of Structural Engineering. 123 (1997) 1454–1461. https://doi.org/10.1061/(ASCE)0733-9445(1997)123:11(1454).

[17] World Housing Encyclopedia -WHE, (n.d.). http://db.world-housing.net/building/10/ (accessed April 4, 2022).

[18] F. Jalayer, R. de Risi, G. Manfredi, Bayesian Cloud Analysis: Efficient structural fragility assessment using linear regression, Bulletin of Earthquake Engineering. 13 (2015) 1183–1203. https://doi.org/10.1007/S10518-014-9692-Z.

[19] FEMA, HAZUS Earthquake Loss Estimation Methodology. Technical Manual, Prepared by the National Ins- titute of Building Sciences for the Federal Emergency Management Agency, Washington D.C., 1999.

[20] FEMA, National Risk Index, Official Website of the Department of Homeland Security. (2021).

[21] H.R. Tavakoli, Probabilistic and Deterministic Seismic Hazard Assessment in Amol Center, a City in North of Iran, Iranica Journal of Energy & Environment. (2012). https://doi.org/10.5829/idosi.ijee.2012.03.03.3004.

[22] A. Coburn, R. Spence, Earthquake Protection, John Wiley & Sons, Ltd, Chichester, UK, 2002. https://doi.org/10.1002/0470855185.

[23] F. de Luca, G.M. Verderame, Seismic Vulnerability Assessment: Reinforced Concrete Structures, in: Encyclopedia of Earthquake Engineering, Springer Berlin Heidelberg, Berlin, Heidelberg, 2015: pp. 3182–3210. https://doi.org/10.1007/978-3-642-35344-4_252.

[24] H. Naderpour, M. Mirrashid, A novel definition of damage states for structural elements in framed reinforced concrete buildings, Journal of Building Engineering. 32 (2020) 101479. https://doi.org/10.1016/j.jobe.2020.101479.

[25] M. Paz, Structures Modeled as Single-Degree-of-Freedom Systems, in: International Handbook of Earthquake Engineering, Springer US, Boston, MA, 1994: pp. 3–9. https://doi.org/10.1007/978-1-4615-2069-6_1.

[26] Earthquake Hazards, Earthquake Magnitude, Energy Release, and Shaking Intensity, USGS Science for a Changing World. (n.d.).

[27] A. Whittaker, G.G. Deierlein, J. Hooper, A. Merovich, Engineering demand parameters for structural framing systems, United States of America, 2004.

[28] H. Dantanarayan, G.A. MacRae, R.P. Dhakal, T.Z. Yeow, S.R. Uma, Quantifying building engineering demand parameters in seismic events., in: Lisbon, Portugal: 15th World Conference on Earthquake Engineering (15WCEE), Lisbon, 2012.

[29] Building Seismic Safety Council, NEHRP Guidelines for the seismic rehabilitation of buildings, Washington D.C., 1997.

[30] Applied Technology Council, ATC-14 Evaluating the seismic resistance of existing buildings, Redwood City, California , 1985.

[31] Applied Technology Council, ATC-22 A Handbook for Seismic Evaluation of Existing Buildings, Redwood City, California , 1988.

[32] C. Kang, O.-S. Kwon, J. Song, Evaluation of correlation between engineering demand parameters of structures for seismic system reliability analysis, Structural Safety. 93 (2021) 102133. https://doi.org/10.1016/j.strusafe.2021.102133.

[33] Red Sismologica Nacional de Colombia, (n.d.). http://bdrsnc.sgc.gov.co/sismologia1/HCG/acelerografos/consultas/Experta_RNAC/index.php (accessed December 9, 2021).

[34] F. Mohamed Nazri, Fragility Curves, in: 2018: pp. 3–30. https://doi.org/10.1007/978-981-10-7125-6_2.

[35] S. Lagomarsino, S. Cattari, D. Ottonelli, The heuristic vulnerability model: fragility curves for masonry buildings, Bulletin of Earthquake Engineering. 19 (2021) 3129–3163. https://doi.org/10.1007/s10518-021-01063-7.

[36] COMSOL, Response Spectrum Analysis, Multyphysics Cyclopedia. (n.d.). https://www.comsol.com/multiphysics/response-spectrum-analysis#:~:text=Response%20spectrum%20analysis%20is%20a,perform%20a%20time%2Ddependent%20analysis. (accessed May 4, 2022).

[37] A. Erman, S.A. de Vries Robbé, S.F. Thies, K. Kabir, M. Maruo, Gender Dimensions of Disaster Risk and Resilience, Washington, DC, 2021.

[38] Å. Löfström, Gender equality, economic growth and employment., 2009.

[39] W. Anderson, Women and Children Facing Disaster, 2nd ed., The World Bank, 2000.

[40] A.M. Thurston, H. Stöckl, M. Ranganathan, Natural hazards, disasters and violence against women and girls: a global mixed-methods systematic review, BMJ Global Health. 6 (2021) e004377. https://doi.org/10.1136/BMJGH-2020-004377.

[41] J. Lynn Ross, V. Gimenez-Pinto, E. del Gado, B. Franco-Orozco, C.M. Franco-Orozco, Women in Academia and Research: An Overview of the Challenges Toward Gender Equality in Colombia and How to Move Forward, Frontiers in Astronomy and Space Sciences | Www.Frontiersin.Org. 1 (2018) 24. https://doi.org/10.3389/fspas.2018.00024.

[42] E. Enarson, Gender and Natural Disasters, Geneva, 2000.

[43] A.K. Shukla, S. Kumar, P.R. Maiti, Failure Analysis of Unconfined Brick Masonry with Experimental Verification, Undefined. 21 (2021) 419–428. https://doi.org/10.1007/S11668-021-01116-8.

[44] E. Alarcón, Benito-Oterino M.B., Mucciarelli M., Liberatore D., Bulletin of Earthquake Engineering - v. 12, n. 5, Structurae. (2013) 1871–2298. https://structurae.net/en/literature/periodicals/bulletin-of-earthquake-engineering/20473-12-5 (accessed November 28, 2021).

[45] L. Martins, V. Silva, Development of a fragility and vulnerability model for global seismic risk analyses, Bulletin of Earthquake Engineering. 19 (2021) 6719–6745. https://doi.org/10.1007/s10518-020-00885-1.

[46] N. Tarque, H. Crowley, R. Pinho, H. Varum, Displacement-Based Fragility Curves for Seismic Assessment of Adobe Buildings in Cusco, Peru, Earthquake Spectra. 28 (2012) 759–794. https://doi.org/10.1193/1.4000001.

[47] L. Martins, V. Silva, Development of a fragility and vulnerability model for global seismic risk analyses, Bulletin of Earthquake Engineering. (2020). https://doi.org/10.1007/s10518-020-00885-1.

[48] Freeman, Development and Use of Capacity Spectrum Method. Proceedings of the 6th U.S. National Conference on Earthquake Engineering, Seattle, Oakland, USA., in: Scientific Research Publishing, 1998. https://www.scirp.org/(S(351jmbntvnsjt1aadkposzje))/reference/ReferencesPapers.aspx?ReferenceID=1773086 (accessed November 28, 2021).

[49] ATC-40, Seismic evaluation and retrofit of concrete buildings, Applied Technology Council, Redwood City, California , 1996.

[50] Comité AIS-300, Estudio General de Amenaza Sismica de Colombia, Colombia , 2009.

[51] Universidad de Los Andes, Asociación Colombiana de Ingeniería Sismica, INGEOMINAS, Sismicidad Colombiana, in: Estudio de Amenaza Sismica de Colombia , Bogotá, 1995.

[52] W.A.S., H.A., B.J.W., B.J. and G.D.N. Haselton C.B., Selecting and Scaling Earthquake Ground Motions for Performing Response-History Analyses , 15th World Conference on Earthquake Engineering, Lisboa, Portugal. (2012).

[53] N. Luco, P. Bazzurro, Does amplitude scaling of ground motion records result in biased nonlinear structural drift responses?, Earthquake Engineering and Structural Dynamics. 36 (2007) 1813–1835. https://doi.org/10.1002/EQE.695.

[54] Y.F. Vargas-Alzate, R. Gonzalez-Drigo, J.A. Avila-Haro, Multi-Regression Analysis to Enhance the Predictability of the Seismic Response of Buildings, Infrastructures (Basel). 7 (2022) 51. https://doi.org/10.3390/infrastructures7040051.

[55] N. Luco, C.A. Cornell, Structure-Specific Scalar Intensity Measures for Near-Source and Ordinary Earthquake Ground Motions, Earthquake Spectra. 23 (2007) 357–392. https://doi.org/10.1193/1.2723158.

[56] M. Grigoriu, Do seismic intensity measures (IMs) measure up, Undefined. 46 (2016) 80–93. https://doi.org/10.1016/J.PROBENGMECH.2016.09.002.

[57] L. Eads, E. Miranda, D.G. Lignos, Average spectral acceleration as an intensity measure for collapse risk assessment, Earthquake Engineering & Structural Dynamics. 44 (2015) 2057–2073. https://doi.org/10.1002/eqe.2575.

[58] A.K. Kazantzi, D. Vamvatsikos, Intensity measure selection for vulnerability studies of building classes, Earthquake Engineering & Structural Dynamics. 44 (2015) 2677–2694. https://doi.org/10.1002/EQE.2603.

[59] M. Kohrangi, P. Bazzurro, D. Vamvatsikos, A. Spillatura, Conditional spectrum-based ground motion record selection using average spectral acceleration, Earthquake Engineering & Structural Dynamics. 46 (2017) 1667–1685. https://doi.org/10.1002/EQE.2876.

[60] Y.F. Vargas-Alzate, L.G. Pujades, J.R. González-Drigo, R.E. Alva, L.A. Pinzón, On the equal displacement aproximation for mid-rise reinforced concrete buildings, in: Proceedings of the 7th International Conference on Computational Methods in Structural Dynamics and Earthquake Engineering (COMPDYN 2015), Institute of Structural Analysis and Antiseismic Research School of Civil Engineering National Technical University of Athens (NTUA) Greece, Athens, 2019: pp. 5490–5502. https://doi.org/10.7712/120119.7321.19849.

[61] Y.F. Vargas-Alzate, A.M. Zapata-Franco, Consequences of gender inequality in the face of earthquake disasters, in: 17th World Conference on Earthquake Engineering, 17WCEE, Sendai, Japan, 2021.

[62] J. Pejovic, S. Jankovic, Selection of Ground Motion Intensity Measure for Reinforced Concrete Structure, Procedia Engineering. 117 (2015) 588–595. https://doi.org/10.1016/j.proeng.2015.08.219.

[63] P. Giovenale, C.A. Cornell, L. Esteva, Comparing the adequacy of alternative ground motion intensity measures for the estimation of structural responses, Earthquake Engineering & Structural Dynamics. 33 (2004) 951–979. https://doi.org/10.1002/eqe.386.

[64] N. Shome, C.A. Cornell, Probabilistic Seismic Demand Analysis of Nonlinear Structures, Stanford Digital Repository, 1999.

[65] A. Güllü, E. Yüksel, C. Yalçın, A. Anıl Dindar, H. Özkaynak, O. Büyüköztürk, An improved input energy spectrum verified by the shake table tests, Earthquake Engineering & Structural Dynamics. 48 (2019) 27–45. https://doi.org/10.1002/eqe.3121.

[66] Y. Cheng, A. Lucchini, F. Mollaioli, Correlation of elastic input energy equivalent velocity spectral values, Earthquakes and Structures. 8 (2015) 957–976. https://doi.org/10.12989/eas.2015.8.5.957.

[67] U. Yazgan, Proposal of energy spectra for earthquake resistant design based on turkish registers, Universidad Politécnica de Cataluña, 2012. https://dialnet.unirioja.es/servlet/tesis?codigo=95317.

[68] G. Housner, Earthquake-resistant limit-state design for buildings, by Hiroshi Akiyama, University of Tokyo Press, 1985. Distributed in the U.S. by Columbia University Press. No. of pages: 372. Price: $55, Earthquake Engineering & Structural Dynamics. 14 (1986) 148–148. https://doi.org/10.1002/eqe.4290140112.

[69] V.V. Bertero, C.H. Uang, Issues and future directions in the use of an energy approach for seismic-resistant of design structures, Nonlinear Seismic Analysis and Design of Reinforced Concrete Buildings. (1992) 11–30. https://doi.org/10.1201/9781482296662-1.

[70] Y. Vargas-Alzate, J. Hurtado, Efficiency of Intensity Measures Considering Near- and Far-Fault Ground Motion Records, Geosciences (Basel). 11 (2021) 234. https://doi.org/10.3390/geosciences11060234.

[71] S.K. Sarma, K.S. Yang, An evaluation of strong motion records and a new parameterA95, Earthquake Engineering & Structural Dynamics. 15 (1987) 119–132. https://doi.org/10.1002/eqe.4290150109.

[72] S.K. Sarma, Energy flux of strong earthquakes, Tectonophysics. 11 (1971) 159–173. https://doi.org/10.1016/0040-1951(71)90028-X.

[73] A. Arias, Measure of Earthquake Intensity , Seismic Design for Nuclear Power Plants. /Hansen, Robert J. (Ed.). Cambridge, Mass. Massachusetts Inst. of Tech. Press (1970). (1970) 438–483.

[74] J.W. Reed, R.P. Kassawara, A criterion for determining exceedance of the operating basis earthquake, Nuclear Engineering and Design. 123 (1990) 387–396. https://doi.org/10.1016/0029-5493(90)90259-Z.

[75] G.W. Housner, Measures of severity of earthquake ground shaking, in: Proc. US Natl. Conf. Earthq. Eng. , 1975: pp. 25–33.

[76] Y.J. Park, A.H.-S. Ang, Y.K. Wen, Damage-Limiting Aseismic Design of Buildings, Earthquake Spectra. 3 (1987) 1–26. https://doi.org/10.1193/1.1585416.

[77] P. Fajfar, T. Vidic, M. Fischinger, A measure of earthquake motion capacity to damage medium-period structures, Soil Dynamics and Earthquake Engineering. 9 (1990) 236–242. https://doi.org/10.1016/S0267-7261(05)80002-8.

[78] S.C. Chapra, Applied numerical methods with MATLAB® for engineers and scientists, Fourth, New York, NY : McGraw-Hill Education, 2018.

[79] N. Tarque, H. Crowley, R. Pinho, H. Varum, Seismic risk assessment of adobe dwellings in Cusco, Peru, based on mechanical procedures | Semantic Scholar, 14th European Conference on Earthquake Engineering Ohrid, North Macedonia. (2010).

[80] A. Preciado, A. Ramirez-Gaytan, J.C. Santos, O. Rodriguez, Seismic vulnerability assessment and reduction at a territorial scale on masonry and adobe housing by rapid vulnerability indicators: The case of Tlajomulco, Mexico, International Journal of Disaster Risk Reduction. 44 (2020) 101425. https://doi.org/10.1016/j.ijdrr.2019.101425.

[81] G. Karanikoloudis, P.B. Lourenço, Structural assessment and seismic vulnerability of earthen historic structures. Application of sophisticated numerical and simple analytical models, Engineering Structures. 160 (2018) 488–509. https://doi.org/10.1016/j.engstruct.2017.12.023.

ANNEX A. CLOUDS OF IM-EDP POINTS CLASSIFIED BY NUMBER OF STORIES

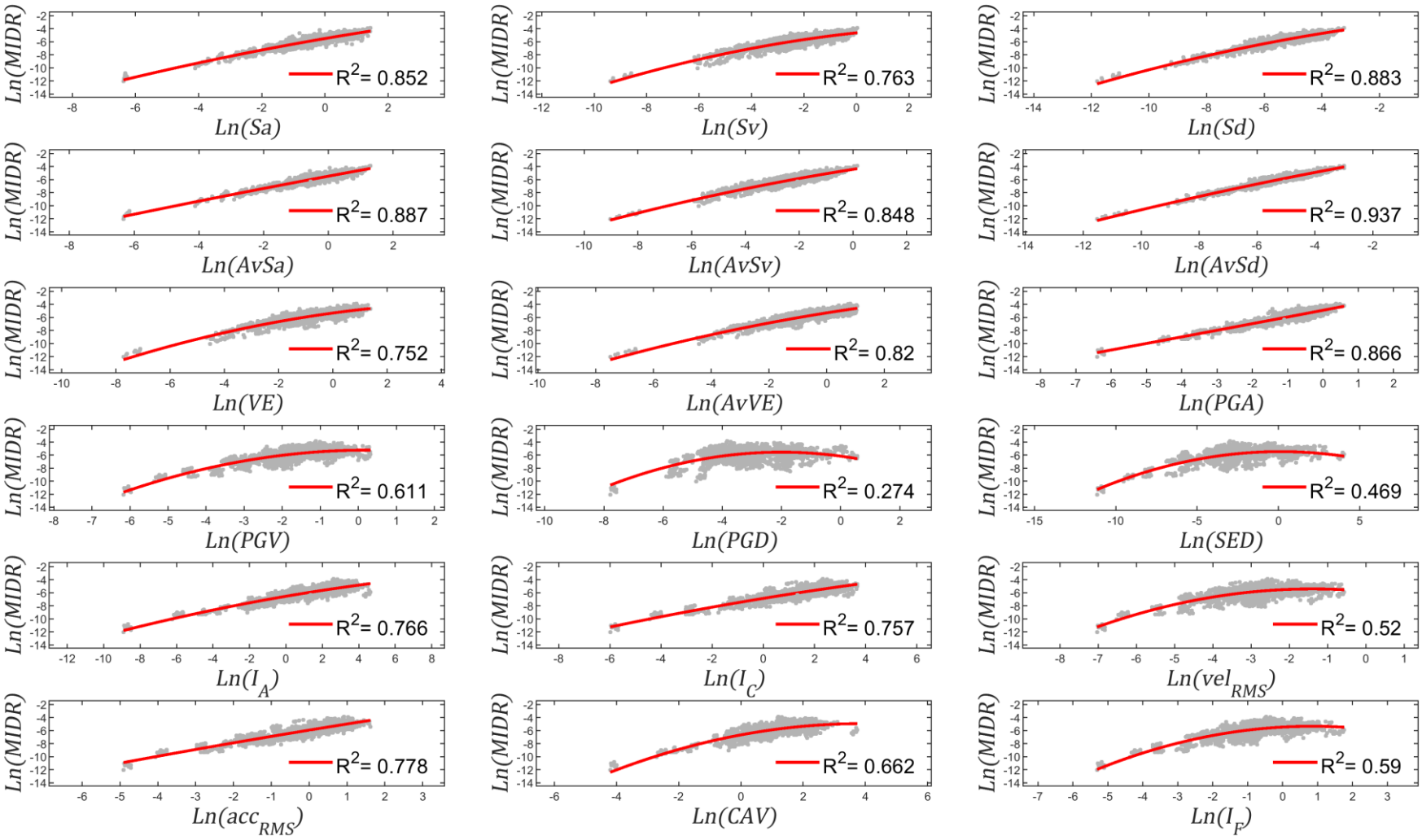

Fig. A-1. Ten-thousand IM-EDP pairs from URMM building models of one story.

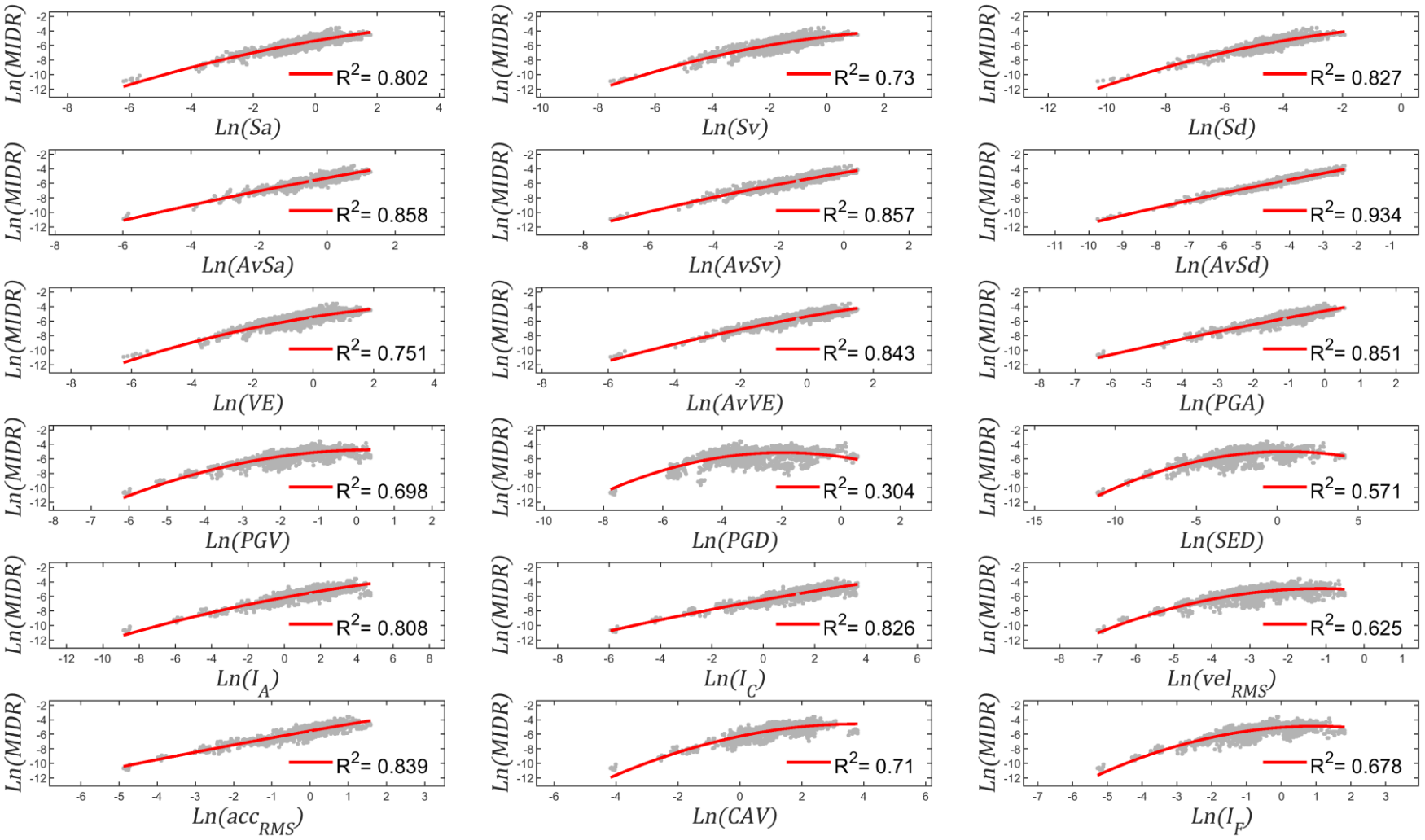

Fig. A- 2. Ten-thousand IM-EDP pairs from URMM building models of two stories.

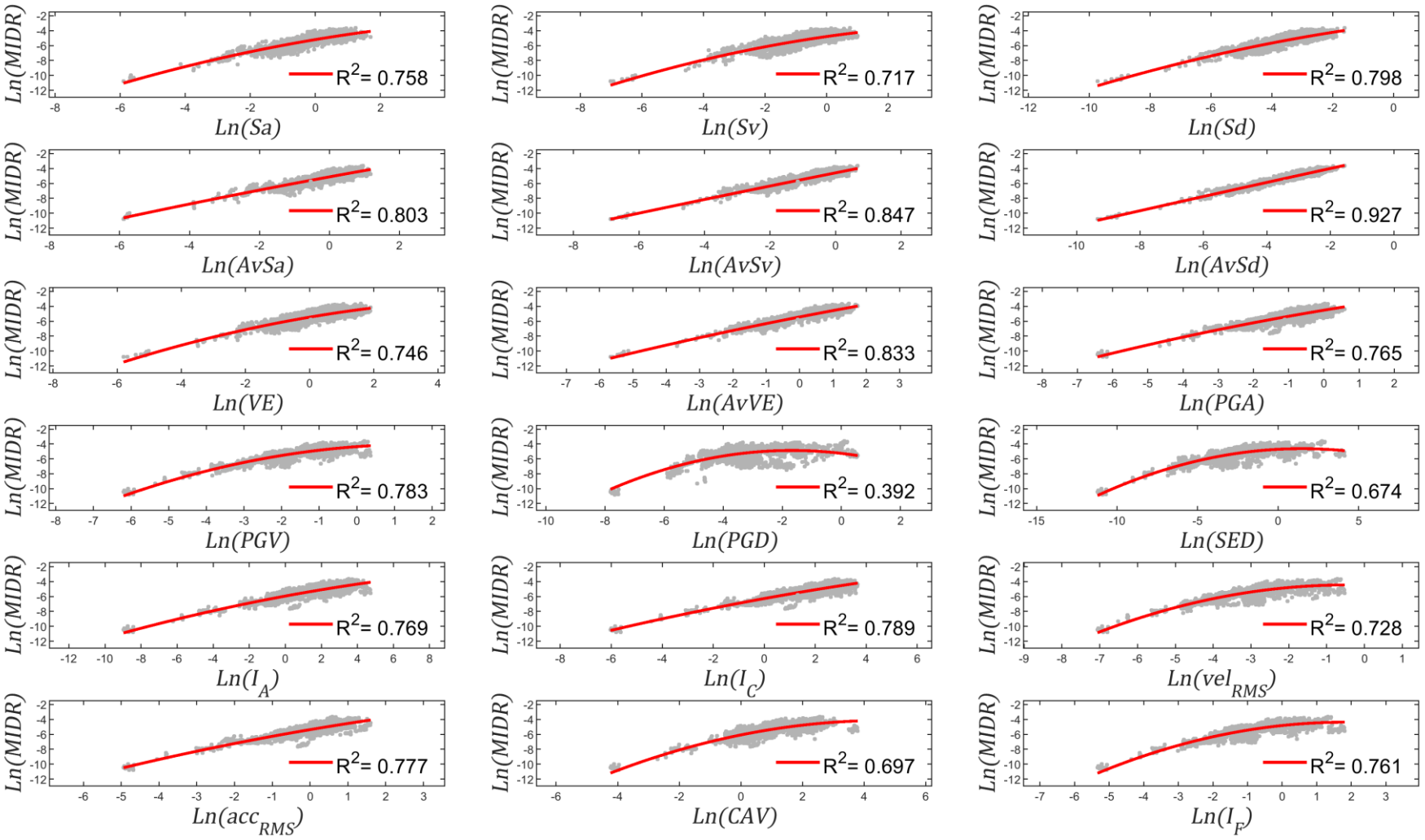

Fig. A- 3. Ten-thousand IM-EDP pairs from URMM building models of tree stories.

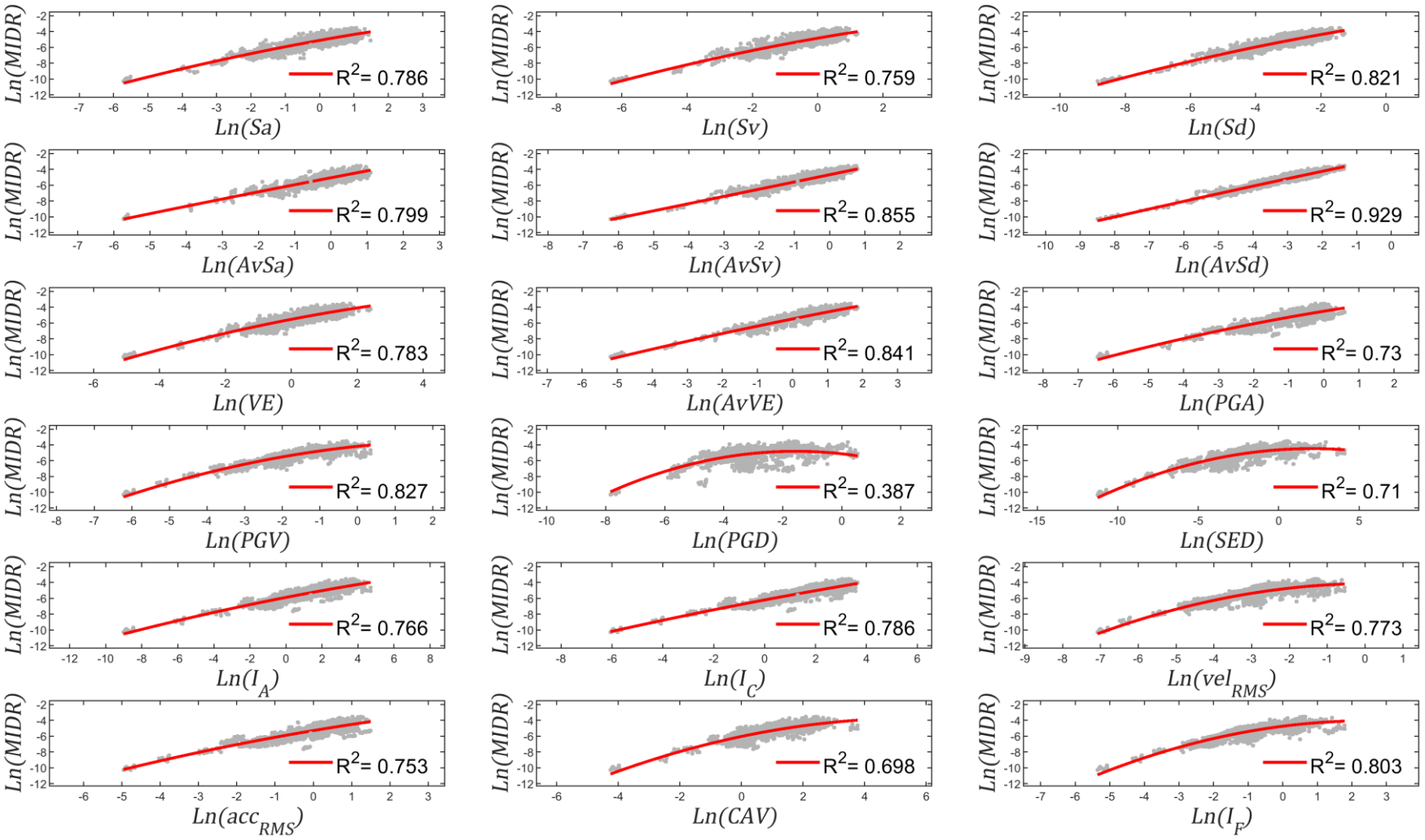

Fig. A- 4. Ten-thousand IM-EDP pairs from URMM building models of four stories.

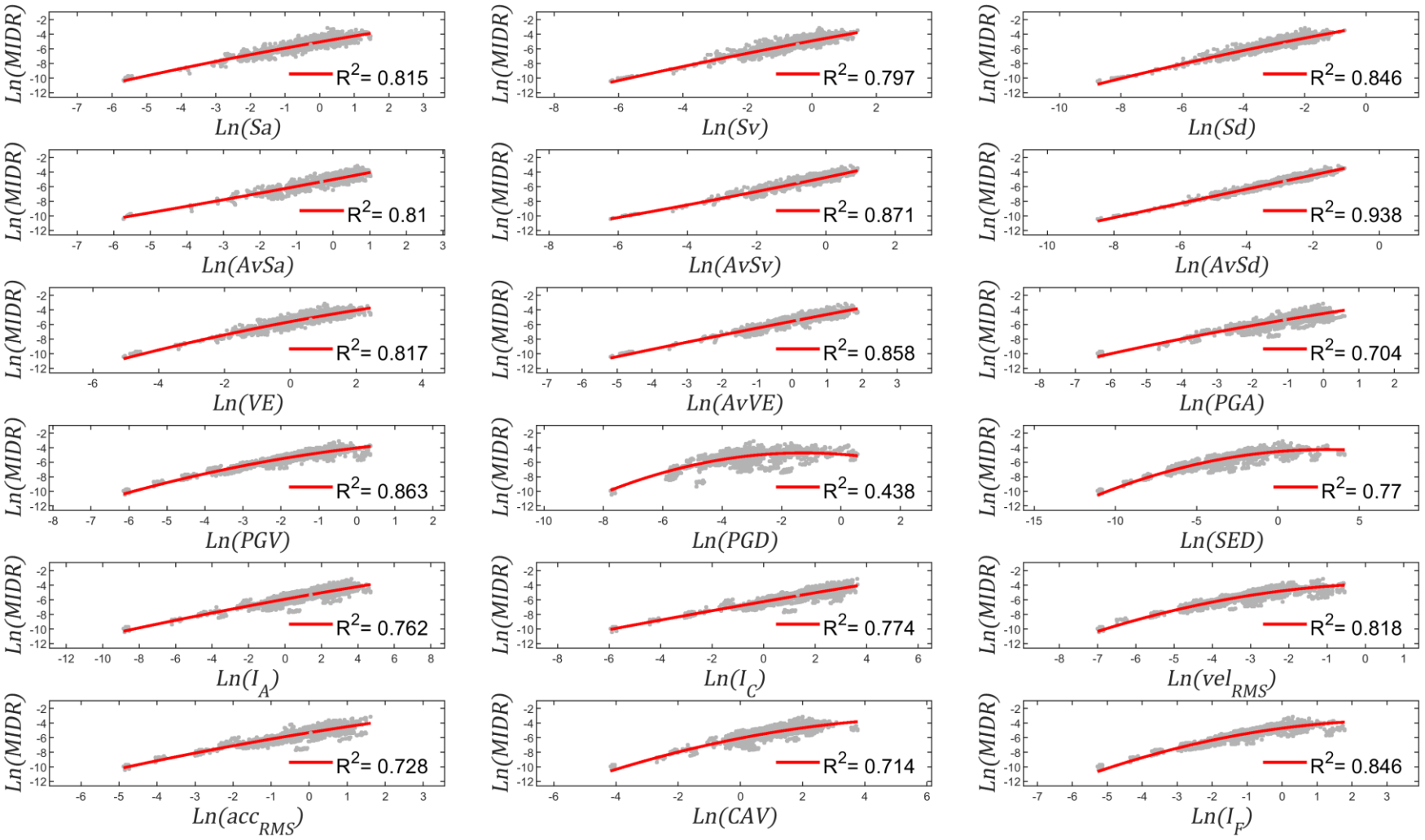

Fig. A- 5. Ten-thousand IM-EDP pairs from URMM building models of five stories.

ANNEX B. NUMBER OF AFFECTED PEOPLE DISCRETIZED BY GENDER, REGION, AND RETURN PERIODS EQUAL TO 475 AND 2475 YEARS.

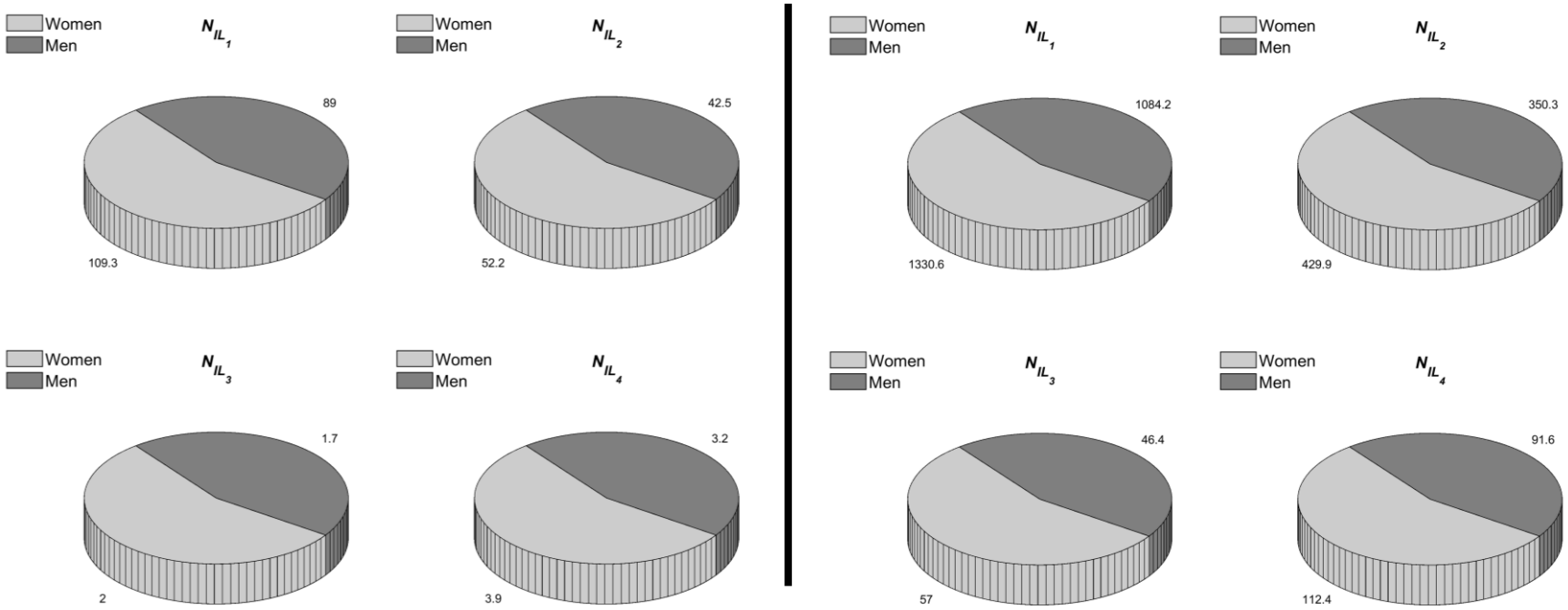

Fig. B- 1. Number of expected women and men affected from Bogotá. Left: Return period of 475 years. Right: Return period of 2475 years

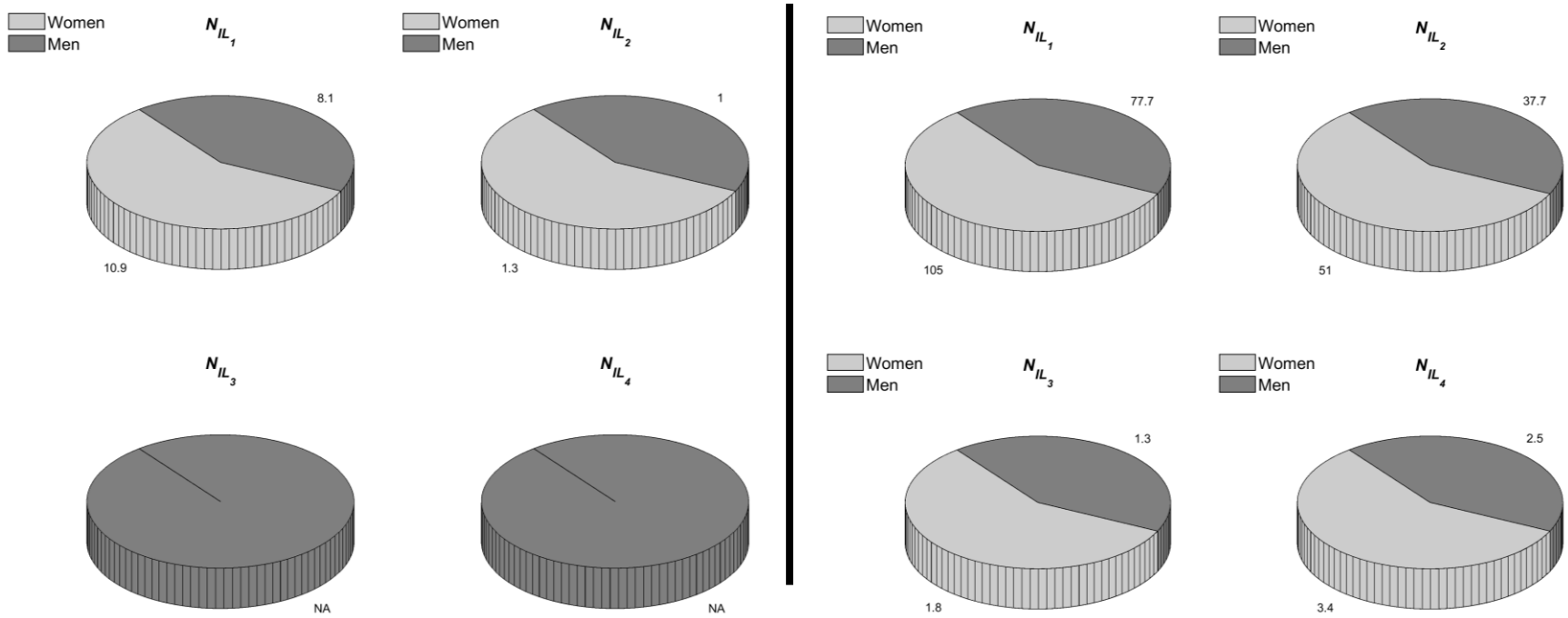

Fig. B- 2. Number of expected women and men affected from Region Caribe. Left: Return period of 475 years. Right: Return period of 2475 years

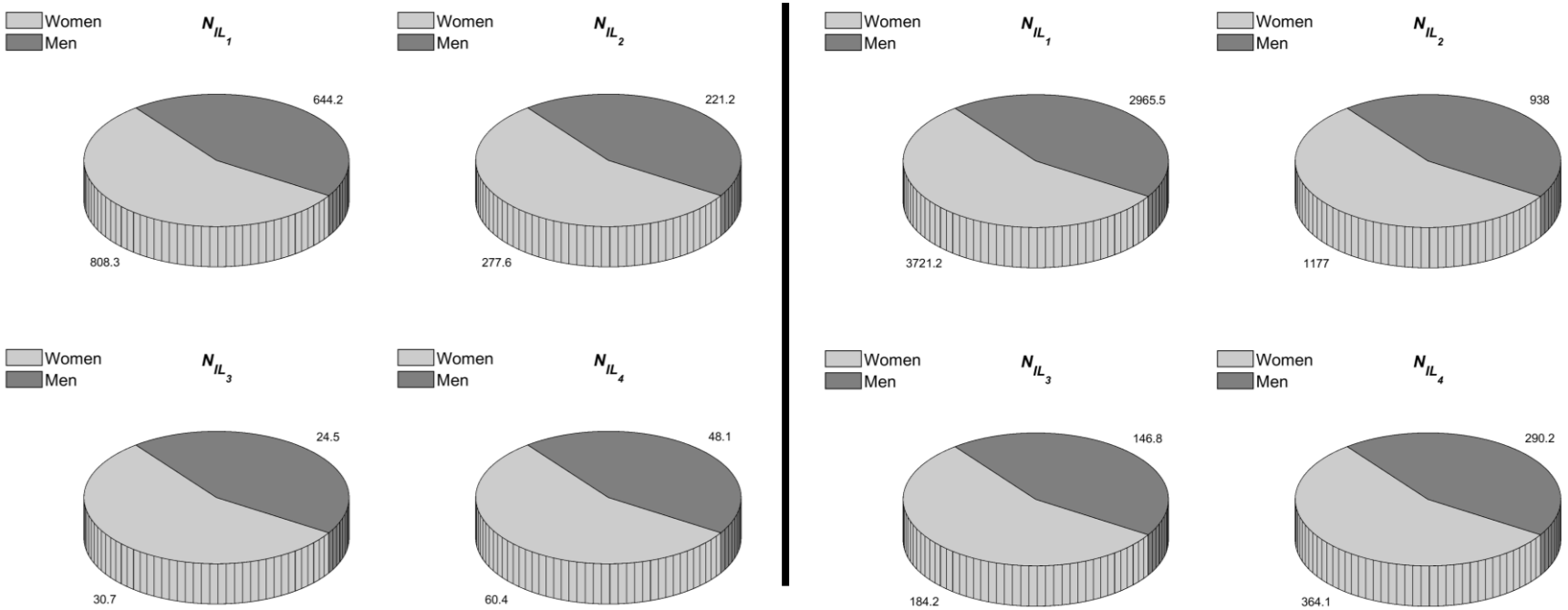

Fig. B- 3. Number of expected women and men affected from Region Central. Left: Return period of 475 years. Right: Return period of 2475 years

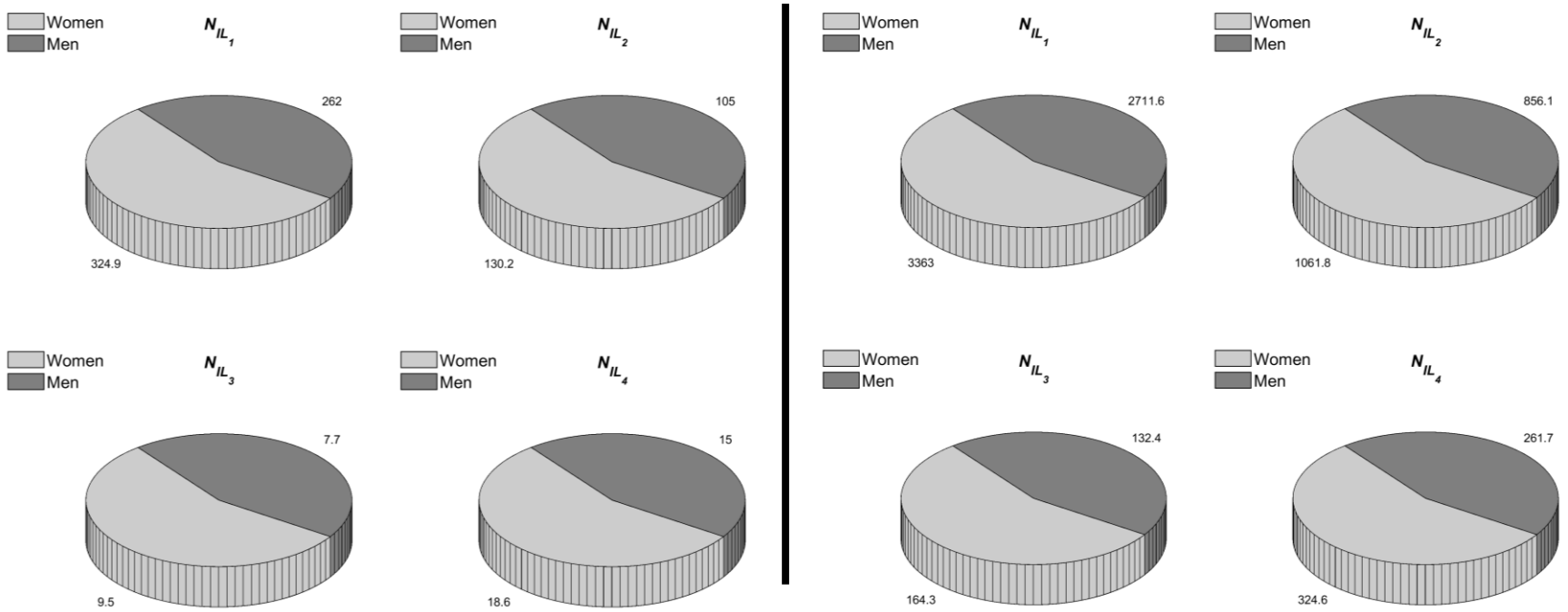

Fig. B- 4. Number of expected women and men affected from Region Oriental. Left: Return period of 475 years. Right: Return period of 2475 years

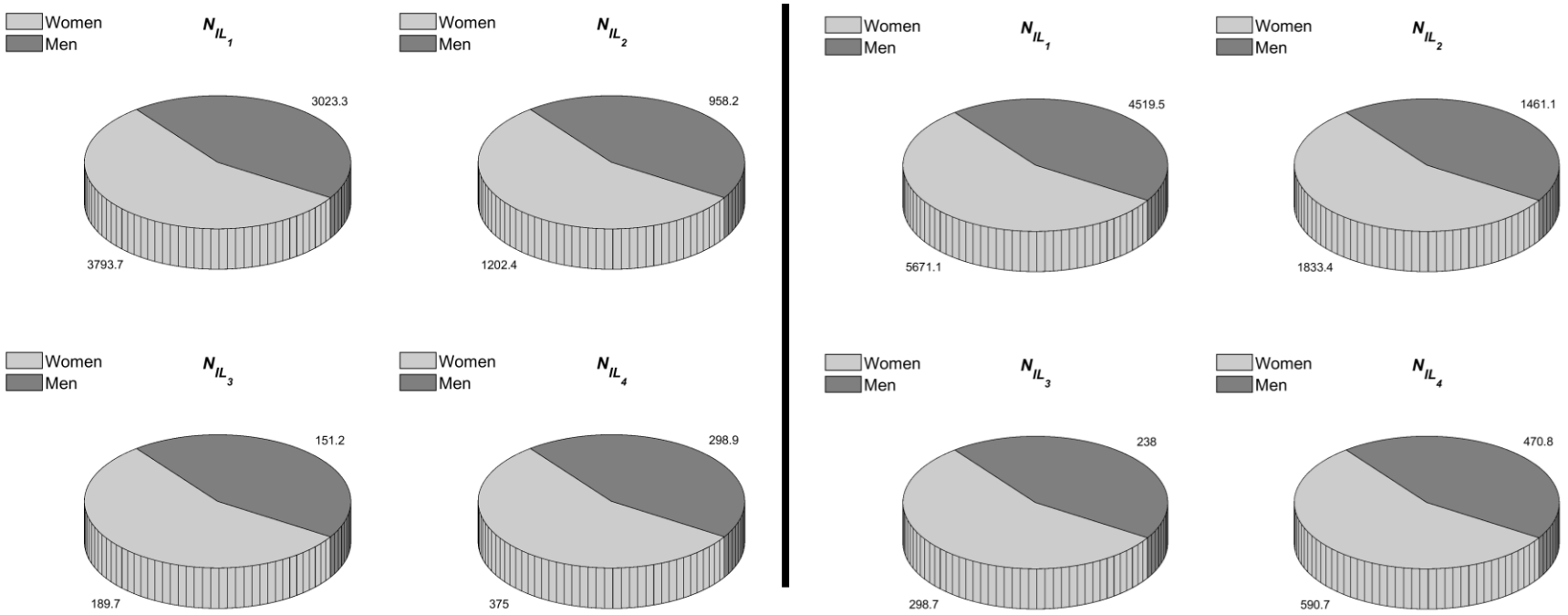

Fig. B- 5. Number of expected women and men affected from Region Pacifica. Left: Return period of 475 years. Right: Return period of 2475 years

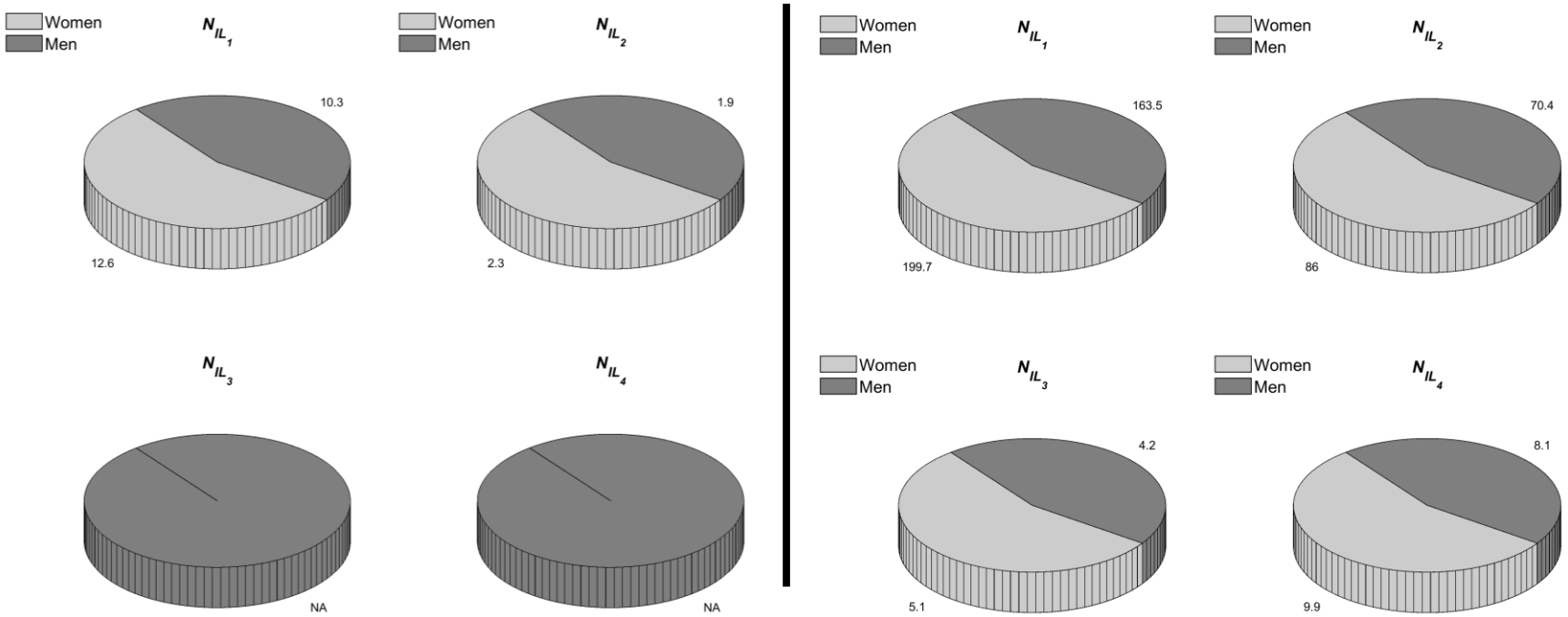

Fig. B- 6. Number of expected women and men affected from Archipelagos. Left: Return period of 475 years. Right: Return period of 2475 years